Understanding Protein Organization in Membranes via Thermodynamic Characterization of Transmembrane Helix Insertion and Association

A thesis report submitted towards the partial fulfillment of

BS-MS Dual Degree Programme

By

Vikas Dubey

Reg. No. 20111008

Under the guidance of **Dr. Durba Sengupta**

Indian Institute of Science Education and Research, Pune

Certificate

This is to certify that this dissertation entitled "**Understanding Protein Organization in Membranes via Thermodynamic Characterization of Transmembrane Helix Insertion and Association**" towards the partial fulfilment of the BS-MS dual degree programme at the Indian Institute of Science Education and Research, Pune represents Original research carried out by **Vikas Dubey** at **CSIR – National Chemical Laboratory, Pune** under the supervision of **Dr. Durba Sengupta**, Ramalingaswami Fellow, **Physical Chemistry Division, National Chemical Laboratory, Pune** during the academic year 2015-2016.

Durba Sengupta

Signature

Date: 28-03-2016

Dr. Durba Sengupta
Scientist Fellow (Ramalingaswami Fellow)
Physical Chemistry Division
National Chemical Laboratory
Dr. Homi Bhabha Road
Pune 411008, India
Phone +91 20 2590 2408
E-mail d.sengupta@ncl.res.in

Declaration

I hereby declare that the matter embodied in the report entitled **"Understanding Protein Organization in Membranes via Thermodynamic Characterization of Transmembrane Helix Insertion and Association"** are the results of the investigations carried out by me at the Department of physical Chemistry, **CSIR- National Chemical Laboratory**, **Pune** under the supervision of **Dr. Durba Sengupta** and the same has not been submitted elsewhere for any other degree.

Vikas

Signature

Vikas Dubey

Date: 28-03-2016

Acknowledgements

I would like to express my sincere gratitude to my supervisor Dr. Durba Sengupta, National Chemical Laboratory (NCL), Pune, who encouraged me for the scientific study that I have carried out at National Chemical Laboratory (NCL), Pune as part of my Master's research project. Her expertise and in depth understanding of the field constantly inspired me throughout to work hard on this challenging research experience. I am gratefully acknowledge her for making me realize the potential in me to pursue research as a career later in my life. I could not have imagined having a better advisor and mentor for my 5th year M.S. project

I thank Dr. Arnab Mukherjee Associate Professor; IISER Pune, who has constantly helped in my Master's thesis project with his valuable feedback and played a major part in making this possible.

I thank my group members Xavier, Aiswarya, Aditi, Shalmali, and Krushna for their constant help throughout the project. Without their immense efforts, It wouldn't have been possible for me learn fundamentals of biology.

I gratefully acknowledges the support of Multi-Scale Simulation and Modeling project – MSM (CSC0129) at CSIR-NCL for providing computational time.

Table of contents

List of figures

List of Tables

Abstract

The insertion and association of membrane proteins are important in several cellular processes. Most of these processes were thought to be protein-driven, but increasing evidence points towards a large role of the membrane. For instance, the “lipophobic” contribution to insertion, analogous to the hydrophobic effect, has been suggested to contribute to the association of membrane peptides. However, the main driving forces have not been thermodynamically quantified. Here, we study the insertion of a polyalanine peptide into a lipid bilayer and estimate the free energy of insertion, as well as the lipophobic component. Free energy calculations have been performed using a coarse-grain force-field for each of the individual coarse-grain beads and polyalanine peptides of increasing length. As expected, the charged and polar moieties have the least favorable free energy of insertion, and the highest lipophobic component. A length-dependence is observed in the polyalanine peptides with the lipophobic component increasing non-linearly with peptide length. The effect of membrane fluidity has been tested by varying temperature and lipid type. The lipophobic contribution increases with decreasing membrane fluidity, although the total free energy of insertion is variable. The results are an important step in estimating the membrane effects in protein insertion and association.

Introduction

Cellular membrane is the outermost layer of the cell membranes. It generally acts as a barrier to serve the purpose of transportation i.e. it regulates the movement of selective substances, e.g. ions and organic molecules in and out of cells and also, shields the cell from the surrounding environment [20]. Cellular membrane generally comprised of a phospholipid bilayer, water and membrane proteins, which are embedded in lipid bilayers. Membrane protein incorporation and

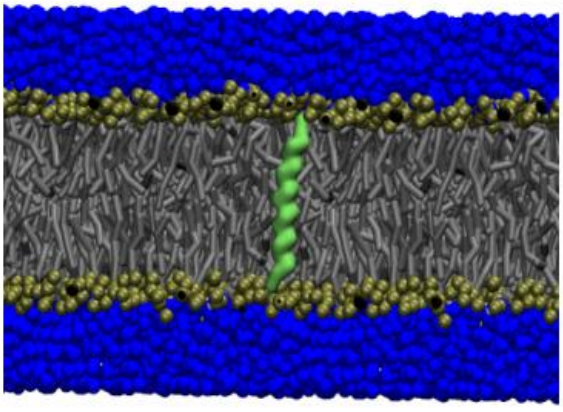

***Figure 1** : Membrane protein (Polyalanine) embedded in a DPPC bilayer*

organization in a lipid bilayer plays an important role in several vital cellular processes, such as transmembrane signaling, adhesion and metabolite transport. Experimental studies due to limited resolution cannot always provide a better understanding of the underlying processes. Hence, to achieve the clearer picture computational studies seems to suit better. These computational tools with the help of statistical mechanics enable us to estimate the macroscopic properties of system e.g. density, thermodynamic free energy.

Thermodynamic free energy is an important thermodynamic property that often estimated to get a better understanding of biological processes. Thermodynamic free energy is generally defined as the energy contained in a system that can be translated into work. It is subdivided in two categories: Helmholtz free energy (A) and Gibbs free energy (G). Helmholtz free energy is the free energy that can be translate into work at constant temperature and volume, Gibbs free energy is the free energy can be transcribed into work at constant temperature and pressure. Biological systems usually deals with constant pressure and temperature conditions, hence Gibbs free energy is a better choice to comprehend the underlying biological processes. Estimating the difference of Gibbs free energy (ΔG) between the states of a system imparts the information about spontaneity of transitions undergoing in the particular process as well as stability of the individual states. Additionally, there are numerous computational methods by which one can evaluate difference of Gibbs free energy accurately. These properties makes Gibbs free energy ideal candidate to investigate detailed energetics of membrane protein insertion and association.

Understanding the detailed energetics of membrane protein insertion and association can provide critical details about various human diseases and viral mechanisms [1][2][3]. Association has been shown to qualitatively depend on different factors e.g. membrane composition, fluidity and curvature. Protein-protein energetics is considered as a major rationale behind membrane protein assembly. However, the thermodynamic contribution of membrane in insertion and consequently association is still not well understood. The role of the hydrophobic effect in the association of the proteins in solution has been well studied [4] . However, the analogous “lipophobic” effect has not been analyzed in detail

and mostly under estimated. The “lipophobic effect”, as described by Jahnig in 1983 [5] is suggested to arise from the penalty of cavity formation in the lipid tails. In a recent publication “orderphobic effect” [6] was suggested as a major driving force for assembly. The authors suggest that lipids have a small contribution in the thermodynamics of incorporation and association of membrane proteins but kinetics is heavily driven by “lipophobic” contribution. In contrast, in a recent article the lipid bilayer is suggested as a major driving force for protein association [7].

Free energy of insertion of polyalanine transmembrane peptides were calculated, together with the membrane contributions. The membrane contributions have been calculated by decomposing the total free energy of insertion into the favorable “lipophilic” and the “lipophobic” components. We estimate the membrane contributions by using molecular dynamics simulations in conjunction with a coarse-grain force-field. The coarse-grain forcefield, MARTINI [8], has been used, despite its lack of atomistic representation, since it has been previously shown to reproduce the energetics of membrane insertion and association. We have first focused on the beads making up the amino acid residues and calculated the energetics for each bead-type at the center of the membrane. Further, the lipophobic contribution in polyalanine peptides of varying lengths was calculated. To test the effect of membrane fluidity, that has been shown to affect membrane protein association, we changed the temperature and lipid type. The lipophobic contribution to membrane peptide insertion and association has been shown to be large and dependent on membrane fluidity.

Computational methods

Molecular Dynamics (MD)

Molecular dynamics is an important algorithm that has been developed to understand time evolution of a system of interacting particles in a particular process. It is governed by Newtonian mechanics. Trajectories of the set of interacting particles is calculated by

solving newton's equations of motion [16] [17] [18]. If the position of the particle kth with mass m_k at time t is $r_k(t) = x_k(t), y_k(t), z_k(t)$ then force can be represented by second order differential equation, shown in eq. (1) [19] [14]

$$F_k = m_k \frac{d^2 r_k(t)}{dt^2} \quad (1)$$

Potential energy (*U*) for a general multi-atom system can be written as eq. (2)

$$U_{system} = U_{bonded} + U_{non-bonded} \quad (2)$$

Bonded interactions, which constitute bonded potential energy, includes all type of bonds presents between two atoms e.g. dihedrals, covalent bonds. Non-bonded interaction consists of Lennard Jones (LJ) interactions i.e. van der Waals interactions and electrostatic interactions [18].

$$F_k = -\frac{dU}{dr_k} \quad (3)$$

A molecular dynamics simulation starts by acquiring initial structure of the system and initial velocities of particles [18]. This information is used to calculate the accelerations and forces between interacting particles. Integration of previously estimated forces leads to the changes in the potential energy of the system [18]. These changes in potential energies provides to a set of possible stable and metastable structures known as microscopic states. Forces between particles are evaluated by integrating the first order differential equation [19] (eq. (3)).These forces, when substituted in newton's equation (eq. (1)), enables us to determine co-ordinates of interacting particles after a certain period of time [18]. Eq. (1), a second order differential equation, is integrated to calculate the trajectories of motion of the particles and by analyzing these trajectories one could easily estimate the fundamental molecular properties. The dynamic occurrences that may affect

the fundamental properties of our system of interest can be directly investigated at the atomic level with the assistance of MD. To determine the properties only initial structure i.e. position vectors of the system need to be supplied. These advantages makes MD simulations very crucial, especially for molecular biology related studies [18].

Thermodynamic integration

Thermodynamic integration is an easy and well recognized method to estimate difference of Gibbs free energies. Thermodynamic integration estimates the free energies between two states by evaluating the potential energies of individual states, since Gibbs free energy is not directly depend on spatial coordinates of the particles of the system. These potential energies with the help of statistical mechanics provides the difference of Gibbs free energies between the states and can be directly obtained by molecular dynamic simulations.

To obtain the numerical relation between free energy and potential energy, we consider two systems M and N having potential energies U_M and U_N.Also, assume the definition of potential energy [12][13][18][21] .

$$U(\lambda) = U_M + \lambda(U_N - U_M) \tag{4}$$

Parameter λ is also known as the coupling parameter having a value between 0 and 1 [12]. It's a measure of all the bonded and non-bonded interactions present between the systems at a particular point of time. Now, partition function for the canonical ensemble i.e. NVT ensemble is represented by the following equation [13][22] .

$$Q(N,V,T,\lambda) = \sum_s e^{-\frac{U_S(\lambda)}{K_B T}} \tag{5}$$

Term $U_s(\lambda)$ corresponds potential at a particular state S. Now, free energy is defined as

$$G(N,V,T,\lambda) = -K_B T \ln Q(N,V,T,\lambda) \tag{6}$$

Now, to estimate the free energy difference (∆G) we will rewrite the equation as the following [12] [13] [22]

$$G_N - G_M \rightarrow \Delta G = \int_0^1 \frac{DG(\lambda)}{d\lambda}\, d\lambda \tag{7}$$

By substituting value of G from eq. (6) in eq. (7) and after differentiation, we will get:

$$\Delta G = -\int_0^1 \frac{K_B T}{Q} \frac{dQ}{d\lambda} d\lambda \tag{8}$$

Again, substitution of Q from eq. (5) with ensemble average followed by a differentiation with respect to λ leads to the following expression [12][13]:

$$\Delta G = \frac{K_B T}{Q} \sum_s \frac{1}{K_B T} \exp\left(\frac{-U_s(\lambda)}{K_B(T)}\right) \frac{dU_s(\lambda)}{d\lambda} d\lambda \tag{9}$$

Eq. (9) can be rewritten as [12][13][21][22][23]

$$\Delta G = \int_0^1 \left\langle \frac{dU(\lambda)}{d\lambda} \right\rangle_\lambda d\lambda \tag{10}$$

Eq. (10) shows the relation between ∆G and potential energy. Essentially, free energy can be estimated by evaluating integration of the ensemble averaged derivatives. This is performed in practice by defining a sequence of λ's, followed by calculation of $\langle dU(\lambda)/d\lambda \rangle$ at each λ, and finally each ensemble average is integrated and summed up to obtain overall free energy difference (∆G). Thermodynamic integration is regarded as one of the most accurate and robust method to estimate free energy. The free energy was estimated by the thermodynamic integration method, implemented in GROMACS v-4.5.5.

Coarse-grain molecular dynamics

Coarse-graining is a molecular modelling method that has been recently evolved in order to bridge the time-scales accessible by atomistic simulations (ns-μs) with experiments (μs-s). In coarse-graining, biological systems are represented with reduced degrees of freedom and fine interactions details are abolished [15]. Generally, a group of atoms is represented as a single particle having all the characteristic properties the associated with the group of atoms [15]. Since, fine interactions details are removed, simulations tend to go rapidly compared to atomistic simulations. One could easily achieve microsecond based attributes of biological systems of higher magnitude with the assistance of coarse-graining technique. There are a couple of forcefields available for coarse-graining. Selection of the correct forcefield for coarse-graining is very crucial, since each forcefield usually focusses on a particular aspect of biological phenomenon. To scrutinize membrane energetics of membrane protein interaction MARTINI forcefield [8] is very well renowned. MARTINI uses 4:1 mapping scheme [8], which means generally 4 big atoms and all the attached hydrogen atoms are modeled as a single particle. These particles are known as beads. These beads are divided into several 4 major categories.

1) **Polar Beads** - Represented by P in the forcefield. These beads generally show attributes of polar molecules e.g. ethanol. It has been divided into five different subtypes P1, P2, P3, P4, and P5. These subtypes are characterized on the basis of polarity. P1 is defined as the least polar and P5 is the most polar among all the polar beads.
2) **Non-Polar/Intermediate Beads** - Represented by N in the forcefield. These beads generally show the attributes of non-polar molecules, which possess ability to interact via hydrogen bond interactions e.g. butanol. It has been divided in to 4 subtypes characterized on the basis of the hydrogen bonding capabilities.
    1) **Nd** - A donor non-polar bead
    2) **Na** - An acceptor non-polar bead
    3) **Nda** - A donor and acceptor non-polar bead
    4) **N0** - Non-polar bead with No hydrogen bonding

3) **Apolar Beads** - Described by C in the forcefield. These beads general show the attributes of extremely non-polar beads e.g. alkyl chains. These beads possess no ability to interact via hydrogen bonds and characterized on the basis of polarity similar to polar beads. C1 is defined as the least apolar and P5 is the most apolar among all the polar beads.
4) **Charged Beads** - Described by Q in the forcefield. These beads general show the characteristic of charged molecules e.g. zwitter ionic form of amino acids. Similar to non-polar beads, charged beads are also divided into 4 subtypes on the basis of their ability to interact via hydrogen bonds. Qd, Qa, Qda represent donor, acceptor, donor-acceptor couple beads respectively. Q0 represents the charged bead no hydrogen bonding abilities.

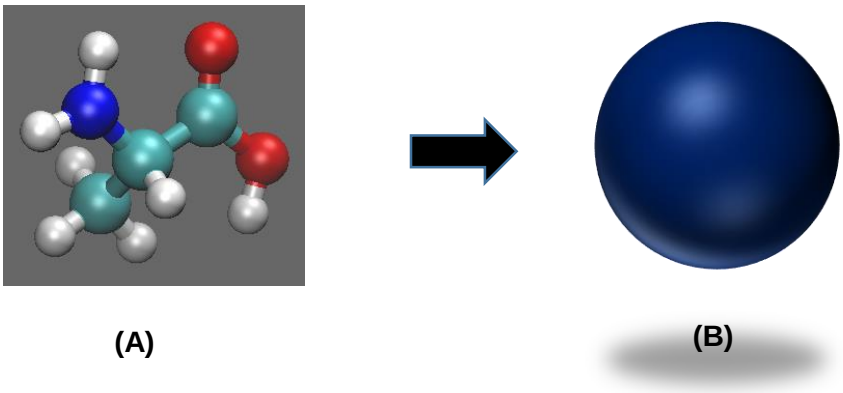

Figure 2 *: Different representations of alanine (A) Atomistic representation (B) Coarse-grain representation*

There are 3 other categories small beads, big beads and aromatic beads, which have been derived from above mentioned bead types. Every aforementioned bead subtype has a corresponding small bead. Only P4 has a corresponding big bead type. C1 and C2 have a corresponding aromatic bead type. There is total of 38 beads in MARTINI. For more details Marrink et al, 2007 [8] can be referred.

Methodology

System setup

Model Polyalanine peptides (Residue 1-30) were embedded in a DPPC bilayer with surrounding water. 10% antifreeze or heavy water was used, as per the requirement of the force-field. In total, 1602 water molecules (including heavy water molecules) and 160 DPPC lipids were present in the system. In the system with DOPC lipids, the peptides were embedded in a DOPC bilayer with surrounding water with 10% antifreeze. Water and lipid composition have been kept the same as in the case of DPPC bilayer.

Peptide	Mixed bead type structure
ALA_1	**P4**
ALA_2	**P4-P4**
ALA_4	**Qd-P4-P4-Qa**
ALA_6	**Qd-N0-N0-N0-N0-Qa**
ALA_8	**Qd-N0-N0-N0-N0-N0-N0-Qa**
ALA_10	**Qd-N0-N0-N0-N0-N0-N0-N0-N0-Qa**
ALA_12	**Qd-N0-N0-N0-N0-C5-C5-N0-N0-N0-N0-N0-Qa**
ALA_14	**Qd-N0-N0-N0-N0-C5-C5-C5-C5-N0-N0-N0-N0-N0-Qa**
↓	**↓ addition of C5 beads at the center**
ALA_30	**Qd-N0-N0-N0-N0-C5-C5-C5-C5-C5-C5-C5-C5-C5-C5-C5-C5-C5-C5-C5-C5-C5-C5-C5-C5-C5-C5-C5-C5-C5-C5-N0-N0-N0-N0-N0-Qa**

Table 1 *: Mixed bead type structures of polyalanine model peptide used in the study.*

Two polyalanine models were tested. Initially, polyalanine was constituted of only C5 bead. In further studies, a more realistic mixed bead type approach was used (Table 1). This mixed bead type structures are determined on the basis of general characteristics of naturally occurring peptides e.g. hydrophobicity, zwitter-ionic structure etc. To calculate the detailed energetics for all of the possible 39 beads individually, the beads were restrained in the middle of the bilayer.

Simulation parameters

Free energy of delipidation/lipidation

We have used GROMACS v-4.5.5 software package for our simulations [9] . Protein, lipid and water were represented by the MARTINI force-field [8]. Stochastic dynamics (sd) integrator was used to carry out free energy calculations. Initially, all the simulations have been carried out at the temperature of 300k and 1 atmospheric pressure. In later, in order to investigate temperature based effect on free energy of delipidation/lipidation as well as on lipophobic contributions, simulations have been performed at 200k temperature as well. Stochastic dynamics (sd) integrator implicitly handles temperature coupling, hence no external thermostat was used. Berendsen barostat [10] was used to ensure pressure coupling. Semiisotropic type pressure coupling scheme was chosen for the simulations. Thermodynamic integration method has been implemented for free energy calculations. Energy penalty of insertion was initially calculated as the free energy of delipidation i.e. free energy required to remove peptide from the membrane. Subsequently, the reverse process (free energy of lipidation) was also calculated. An external restraint along the Z axis with force constant value of 1000 was applied during the simulations, in order to prevent motion along the Z direction. GROMACS parameter pull init1 was used to generate the configurations with different membrane depths. Initially systems were minimized using steepest descent algorithm for 100ps then again minimization was done with Broyden Fletcher Goldfarb Shanno (BFGS) algorithm for another 100ps.It was followed by NVT equilibration for 200ps and then NPT equilibration for another 200ps. All

the production runs have been done for 100ns with $d\lambda$ = 0.05 equispaced 21 λ's between 0 and 1.

Lipophobic contribution

To estimate the lipophobic contribution i.e. the cost of cavity formation for in the process of peptide insertion, attraction term of LJ potential (C6 term) in topology files was switched off. Further, a normal procedure to estimate the free energy of delipidation/lipidation was performed starting from switched off attraction term of LJ potential (C6 term). The methodology was similar to a recent study by Hajari et al [11]. These calculations allow the estimation of the lipophobic contribution in free energy of peptide delipidation/lipidation. The total free energy of insertion, can be decomposed as:

$$DG_{Delipidation/lipidation} = DG_{Lipophobic} + DG_{Lipophilic}$$

If attraction term is switched off, then $DG_{Lipophilic}$ can be considered to be zero. Hence,

$$DG_{Delipidation/lipidation} = DG_{Lipophobic}$$

Results and discussion

In this work we have calculated the free energy of insertion into a lipid bilayer ($\Delta G_{insertion}$) and the lipophobic contribution (ΔG_{LC}). Both the values were estimated by coupling (*i.e.* lipidation, LP) and decoupling (*i.e.* delipidation, DL) the environment, as well as taking the intramolecular coupling (IC) into consideration. As a result, several energy terms have been used in the work and the main abbreviations/symbols used for the different energy terms are mentioned in Table 2.

Abbreviation	Explanation
ΔG_{DL}	Free energy of delipidation i.e. free energy required to take the peptide from lipid environment to vacuum.
ΔG_{LP}	Free energy of lipidation i.e. free energy required to take the peptide from vacuum to lipid environment.

$\Delta G_{DL} - \Delta G_{IC}$	Free energy of delipidation after subtracting the contribution from intramolecular interactions present in peptide.
$\Delta G_{LP} - \Delta G_{IC}$	Free energy of lipidation after subtracting the contribution from intramolecular interactions present in peptide.
ΔG_{DLLC}	Lipophobic contribution i.e. the cost of cavity formation for free energy of delipidation
ΔG_{LPLC}	Lipophobic contribution i.e. the cost of cavity formation for free energy of lipidation
$\Delta G_{DLLC} - \Delta G_{IC}$	Lipophobic contribution for free energy of delipidation after subtracting the contribution from intramolecular interactions.
$\Delta G_{DLLC} - \Delta G_{IC}$	Lipophobic contribution for free energy of lipidation after subtracting the contribution from intramolecular interactions.

Table 2 : *List of symbols used for different free energies terms.*

Energetics of individual MARTINI coarse-grain beads

To begin the investigation of energetics of insertion of polyalanine, we started off by performing simulations with a single bead fixed at the center of the bilayer. We did a detailed analysis of ΔG_{DL}, ΔG_{LP}, ΔG_{DLLC}, ΔG_{LPLC} for all the beads types and subtypes defined in MARTINI forcefield (Table 2). Fig. 3 (A) and (B) shows the ΔG_{DL} and ΔG_{LP} for all major types and subtypes in the order of their decreasing polarity. Most evident conclusion that can be drawn from the Fig. 3 (A) and (B) is that beads with higher polarity i.e. charged beads (Q) and polar beads (P) don't favor to stay at the center of bilayer. On the other hand, beads with lower polarity i.e. non-polar beads (N) and apolar beads (C) seem to be quite stable at the center of bilayer. Due to the favorable van der Waals interactions, non-polar beads (N) and apolar beads (C) tend to interact more with the lipids tails. These interactions allow them to stay at the center of the bilayer. Charged beads (Q) and polar beads (P) are unfavorable at the lipid bilayer center due to their polarity.

Fig. 3 (C) and (D) represents the lipophobic contributions i.e. ΔG_{DLLC} and ΔG_{LPLC} for individual bead types placed at the center of bilayer. This contribution arises from repulsive van der Waals interactions between peptide and lipids tails. Therefore, the lipophobic effect can also be referred as the cost of cavity formation in the membrane environment.

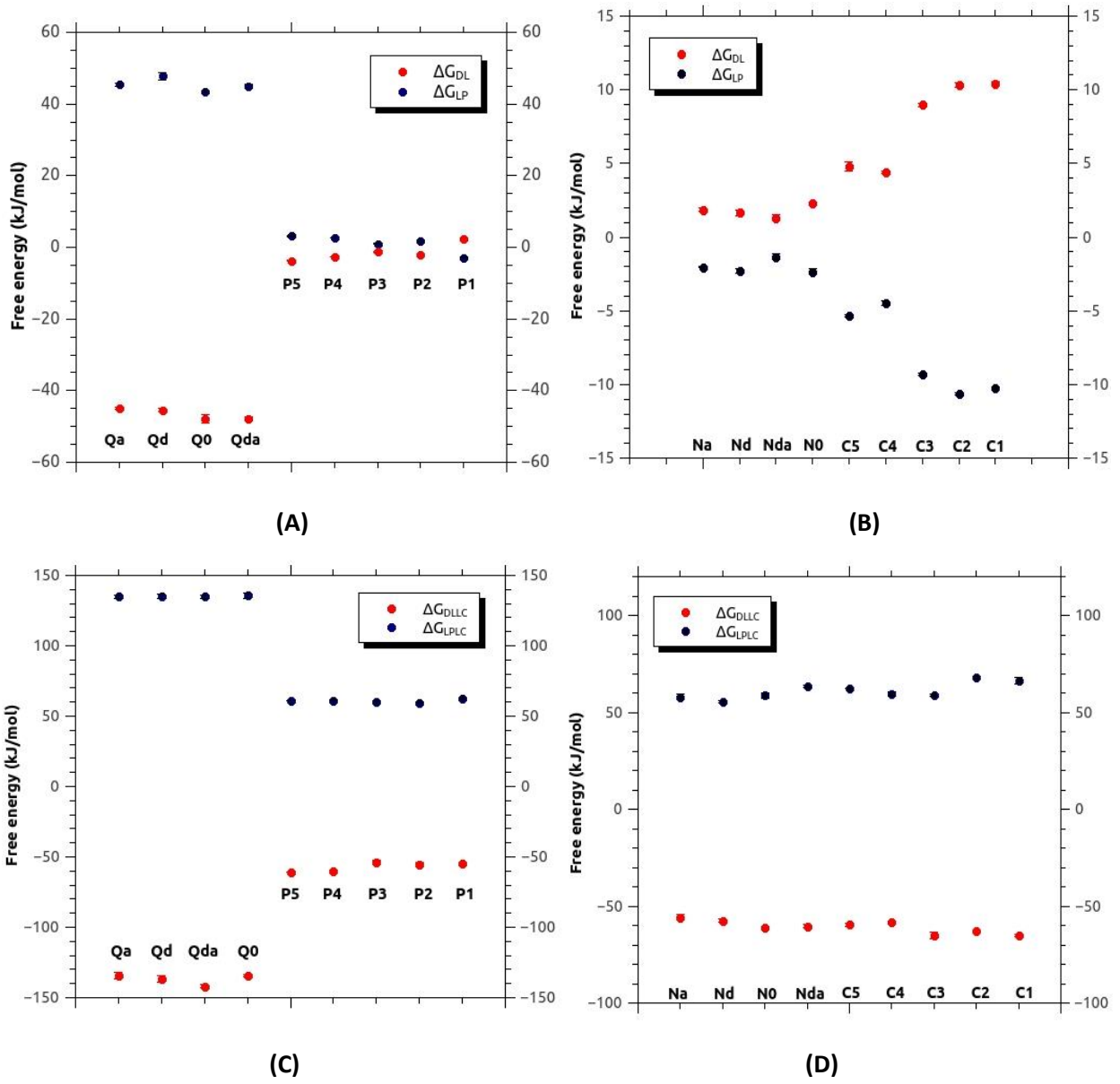

***Figure 3** : **(A)** ΔG_{DL} and ΔG_{LP} for charged (Q) and polar bead (P) types **(B)** ΔG_{DL} and ΔG_{LP} for intermediate/non polar (N) and apolar bead (C) types **(C)** ΔG_{DLLC} and ΔG_{LPLC} for charged (Q) and polar bead (P) types **(D)** ΔG_{DLLC} and ΔG_{LPLC} for intermediate/non polar (N) and apolar bead (C) types, at 300k with DPPC bilayer.*

It is evident from the Fig. 3 (C) that values for ΔG_{DLLC} and ΔG_{LPLC} in the case of charged beads subtypes are highest among all of the bead types, which supports the higher values of ΔG_{DL} and ΔG_{LP} for charged bead types (Q). However, values for ΔG_{DLLC} and ΔG_{LPLC} for polar (P), intermediate (N) and apolar (C) bead types aren't very different from each other (Spp. Table 1). This indicates that membrane effects are similar in these bead types.

Energetics of polyalanine peptides: Single bead type

ΔG_{DL} was estimated for different lengths of polyalanine (residues varying from 1 - 30) with a constant bead type C5. C5 bead is used in MARTINI model to represent an alanine in the center of long α - helix. The free energy of insertion as a function of peptide length is shown in Fig. 4 (A). This shows mostly a linear relationship between number of residues and ΔG_{DL}. A kink around residues 26 corresponds to the peptide spanning in membrane core/acyl chain region. ΔG_{LP} was also estimated and plotted with number of residues to ensure the reversibility of the method, which turned out to be mostly linear. Kink around residues 26 is retained in the plot of ΔG_{LP}. For residues > 2, ΔG_{DL} and ΔG_{LP} has significant contribution of ΔG_{IC}. Hence, ΔG_{DL} was again estimated and plotted after removing the contribution from ΔG_{IC}. Values were examined and plotted by removing the contribution from ΔG_{IC} from ΔG_{LP} as well. Again, relationship between number of residues and free energies after subtracting the ΔG_{IC}, was found to be mostly linear and kink observed around residue 26 remains consistent in the plots of $\Delta G_{DL} - \Delta G_{IC}$ and $\Delta G_{LP} - \Delta G_{IC}$. Additionally to confirm, ΔG_{IC} was estimated by performing free energy calculations for polyalanine in vacuum. From Fig. 4(A) and (B) it is clear that ΔG_{DL} and ΔG_{LP} for single bead type (C5 bead only) model peptide polyalanine increases with number of residues. This suggests that longer peptides containing only C5 bead are more stable in the lipid environment. This can be possibly associated with the increased ability of longer peptides to interact with lipid tails. For estimated values ΔG_{DL}, ΔG_{LP}, $\Delta G_{DL} - \Delta G_{IC}$ and $\Delta G_{LP} - \Delta G_{IC}$ Spp. Table 2 can be referred.

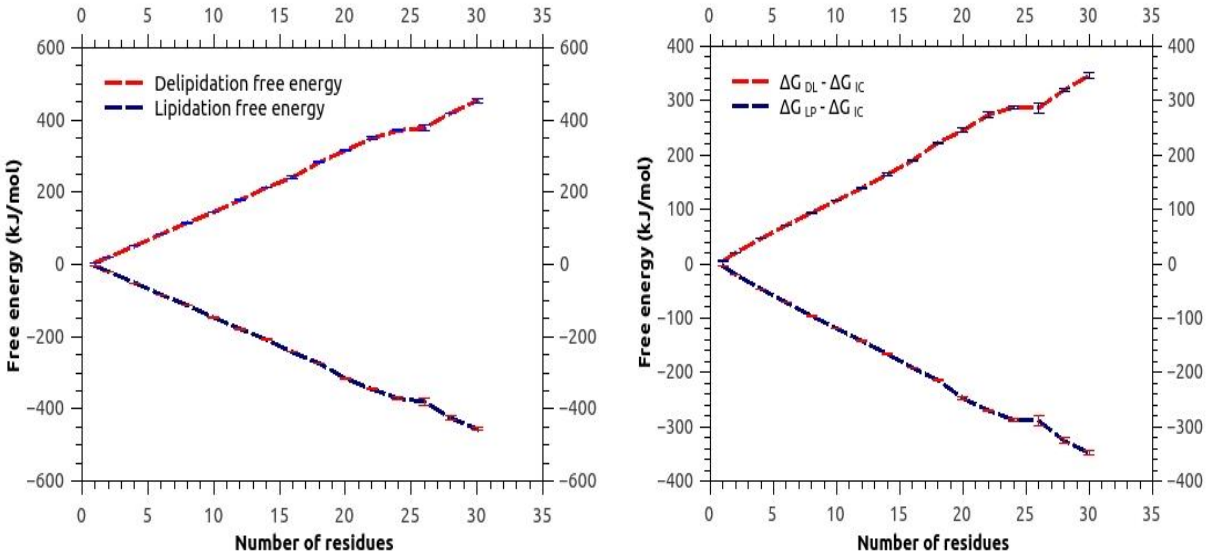

(A) **(B)**

Figure 4 : (A) *variation in* ΔG_{DL} *and* ΔG_{LP} *with number of residues of single bead type polyalanine* ***(B)*** *variation in* ΔG_{DL} - ΔG_{IC} *and* ΔG_{LP} - ΔG_{IC} *with number of residues of single bead type polyalanine (C5 bead only) in kJ/mol, at 300k with DPPC bilayer.*

Lipophobic contributions

We performed simulations for similar set of structures in order to estimate the repulsive contributions i.e. ΔG_{DLLC} and ΔG_{LPLC} and ΔG_{IC} contributions were subtracted in order to correct the overestimation. Both ΔG_{DLLC} - ΔG_{IC} and ΔG_{LPLC} - ΔG_{IC} increase with number of residues as the hydrophobic nature of peptide increases by addition of apolar C5 beads, (Fig. 5(B)). Interestingly, values don't seem to increase by constant amount as it was observed in the case of ΔG_{DL} - ΔG_{IC} and ΔG_{LP} - ΔG_{IC}. Rate to increment becomes lower as we move to ALA_16. Also, a small decay is also observed at ALA_30 in each case. For estimated values ΔG_{DLLC}, ΔG_{LPLC}, ΔG_{DLLC} - ΔG_{IC} and ΔG_{LPLC} - ΔG_{IC} Spp. Table 3 can be referred.

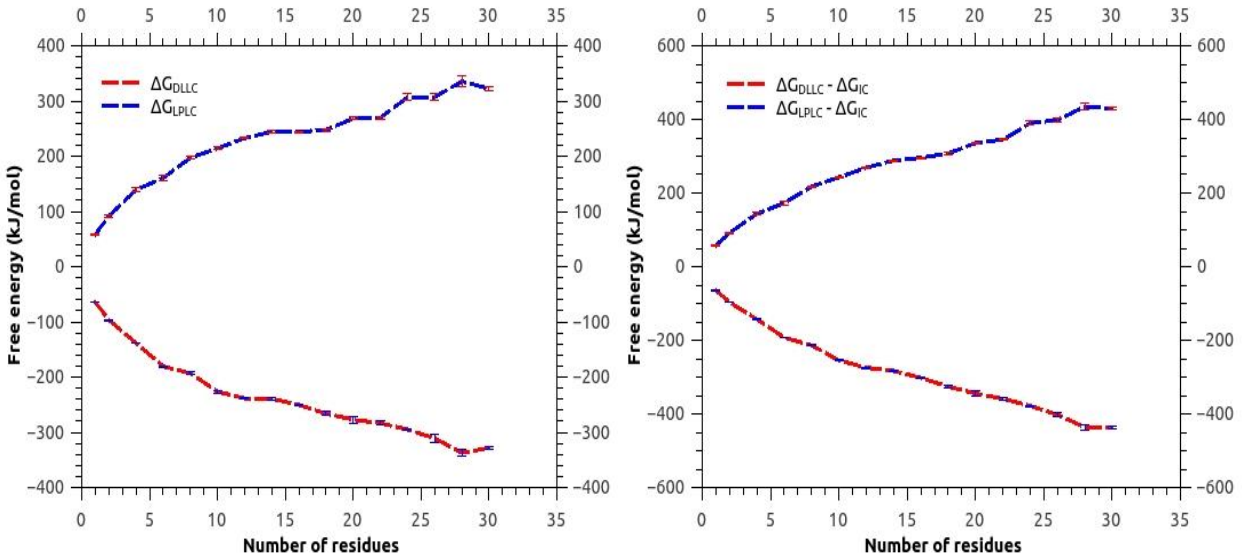

Figure 5: *variation in ΔG_{DLLC} and ΔG_{LPLC} with number of residues of single bead type polyalanine* ***(B)*** *variation in ΔG_{DLLC} - ΔG_{IC} and ΔG_{LPLC} - ΔG_{IC} with number of residues of single bead type polyalanine (C5 bead only) in kJ/mol, at 300k with DPPC bilayer.*

Energetics of polyalanine peptides: Mixed bead type

Simulations were also performed with mixed bead type structures of polyalanine (Table 1). At first, free energies were estimated including both electrostatic (q) and van der Waals interactions (Vdw) present among MARTINI beads (Spp. Table 4). Variation of ΔG_{DL} - ΔG_{IC} and ΔG_{LP} - ΔG_{IC} with different lengths of polyalanine is shown in the Fig. 6(A). Here, ΔG_{DL} - ΔG_{IC} and ΔG_{LP} - ΔG_{IC} don't seem to vary linearly with number of residues. Critical examining of diagrams Fig. 6(A) and (B) suggests that there is a crossover at ALA_5. Also, after ALA_10 values seem to increase at a faster rate until ALA_20. ALA_20 onwards, curve starts to decay slowly until ALA_30. These observations can be explained on the basis of structures of peptides (Table 1). Until ALA_10 peptide is highly polar in nature, due to the presence of N, P, and Q type of beads. ALA_12 onwards, peptide starts to gain apolar character due to addition of C5 beads at the center of peptide. The electrostatic interactions between polar head groups and charged ends of peptide become more prominent and favorable. ALA_22 onwards, non-polar beads (N0 beads) starts to come near to charged head groups, hence chances of van der Waals interactions decreases. This causes a decay in the increment rate of ΔG_{DL} - ΔG_{IC} and ΔG_{LP} - ΔG_{IC}.

This similar process was further repeated to estimate the individual contribution from van der Waals interactions. Simulations were performed including only van der Waals interactions (Vdw) (Spp. Table 5). Contributions from van der Waals interactions mostly vary in a linear fashion with number of residues (Fig. 6(B)). This indicates that parabolic nature of Fig. 6(A) is mostly due to the electrostatic interactions.

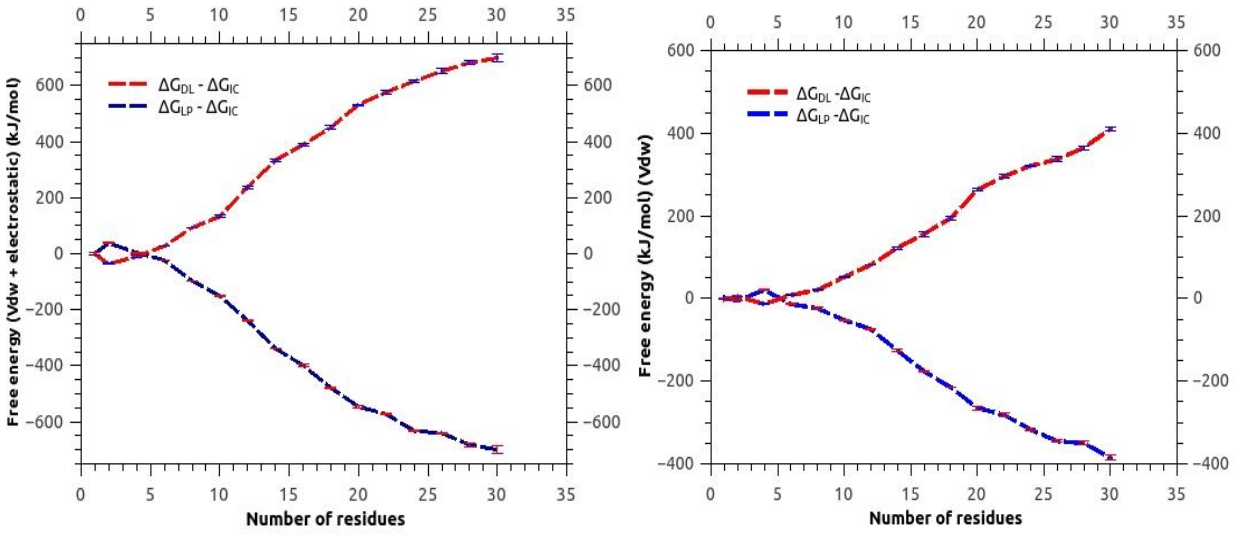

(A) **(B)**

Figure 6 : (A) *variation in ΔG_{DL} - ΔG_{IC} and ΔG_{LP} - ΔG_{IC} with number of residues including both van der Waals and electrostatic interactions* ***(B)*** *variation in ΔG_{DL} - ΔG_{IC} and ΔG_{LP} - ΔG_{IC} with number of residues including only van der Waals interactions, with mixed bead type polyalanine (Table 1) in kJ/mol, at 300k with DPPC bilayer.*

Lipophobic contributions

Lipophobic contributions i.e. cost of cavity formation were estimated for mixed bead type polyalanine including both of including both electrostatic (q) and van der Waals interactions (Vdw) followed by subtraction of ΔG_{IC} (Spp. Table 6). ΔG_{DLLC} - ΔG_{IC} and ΔG_{LPLC} - ΔG_{IC} increases with high increment rate till ALA_10 due to highly polar nature of structure of polyalanine. At ALA_12, there is a drastic decrement in ΔG_{DLLC} - ΔG_{IC} and ΔG_{LPLC} - ΔG_{IC} due to the insertion of apolar C5 beads in the structure (Fig. 7 (A)). This enables peptide to interact with lipid environment by van der Waals interactions. Van der Waals interactions becomes more favorable with further additions apolar C5 beads. This

explain the increment in the values of $\Delta G_{DLLC} - \Delta G_{IC}$ and $\Delta G_{LPLC} - \Delta G_{IC}$ ALA_12 onwards. For the estimated values ΔG_{DLLC}, ΔG_{LPLC}, $\Delta G_{DLLC} - \Delta G_{IC}$ and $\Delta G_{LPLC} - \Delta G_{IC}$ Spp. Table 6 can be referred.

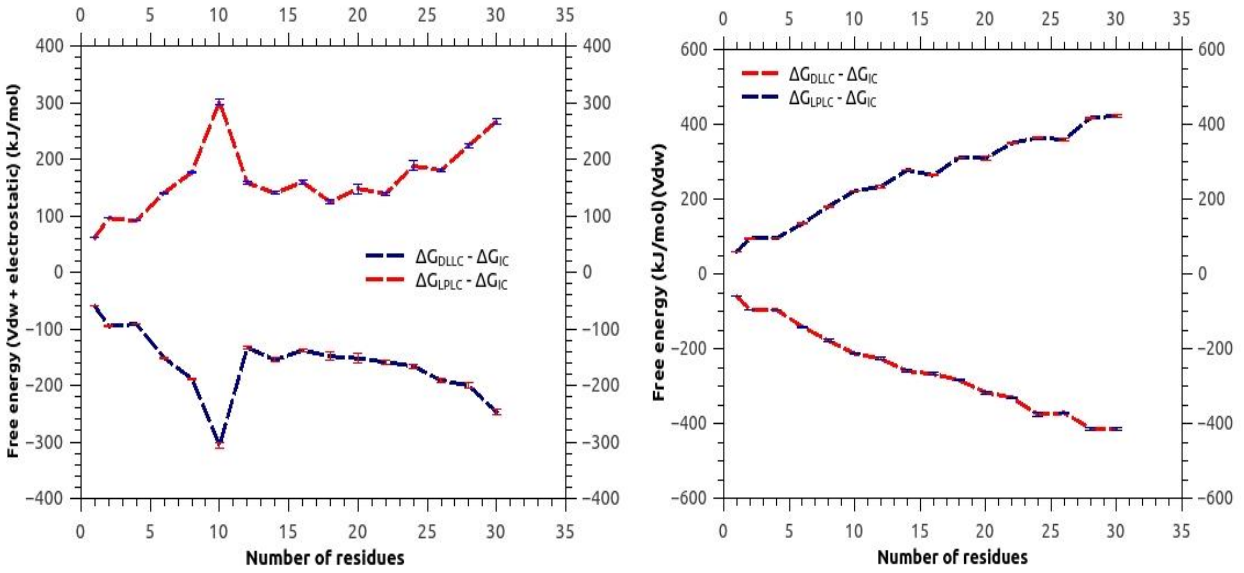

(A) **(B)**

Figure 7 : (A) *variation in $\Delta G_{DLLC} - \Delta G_{IC}$ and $\Delta G_{LPLC} - \Delta G_{IC}$ with number of residues including both van der Waals and electrostatic interactions* ***(B)*** *variation in $\Delta G_{DLLC} - \Delta G_{IC}$ and $\Delta G_{LPLC} - \Delta G_{IC}$ with number of residues including only van der Waals interactions, with mixed bead type polyalanine (Table 1) in kJ/mol, at 300k with DPPC bilayer.*

Further, lipophobic contributions were also for estimated for mixed bead type polyalanine including only van der Waals interactions (Spp. Table 7). Variation of $\Delta G_{DLLC} - \Delta G_{IC}$ is shown in Fig. 7 (B). The increasing hydrophobic character favors the van der Waals interaction in the peptide structure. This possibly explanation that could be associated with the increment in $\Delta G_{DLLC} - \Delta G_{IC}$ and $\Delta G_{DLLC} - \Delta G_{IC}$. Since, electrostatics contribution is excluded in the simulations, involvement of charges causes we find no sudden deflection in curve and graph increases mostly in a linear and smooth fashion.

Analyzing the effect of Membrane Fluidity

Simulations were performed at lower temperature 200 K, at this temperature membrane become more ordered and gel like compared to 300 K. Further, we performed the calculations with a new DOPC bilayer, which is less ordered and more fluid in nature. Details results for both of the cases will be discussed in this section.

Energetics of Polyalanine peptides in DPPC at 200 K

Values of ΔG_{DL} - ΔG_{IC} and ΔG_{LP} - ΔG_{IC} are found to be increasing as observed at 300 K. interestingly (Spp. Table 8), it can be clearly seen in the Fig. 8 (A) and Fig. 8 (B) that the values of ΔG_{DL} - ΔG_{IC} and ΔG_{LP} - ΔG_{IC} are elevated compared to 300k except ALA_4 and ALA_6, which nearly have similar values at both of the temperatures. Although, increment in the values of ΔG_{DL} - ΔG_{IC} and ΔG_{LP} - ΔG_{IC} is have clear trend. There is sharp decay in the values as peptide length approach to membrane core/acyl chain region. The individual contribution from the van der Waals interactions were also observed to have elevated values except for ALA_1 and ALA_2 (Fig. 8 (C) and Fig. 8 (D)), which are mostly similar for the both of the temperatures (Spp. Table 9).

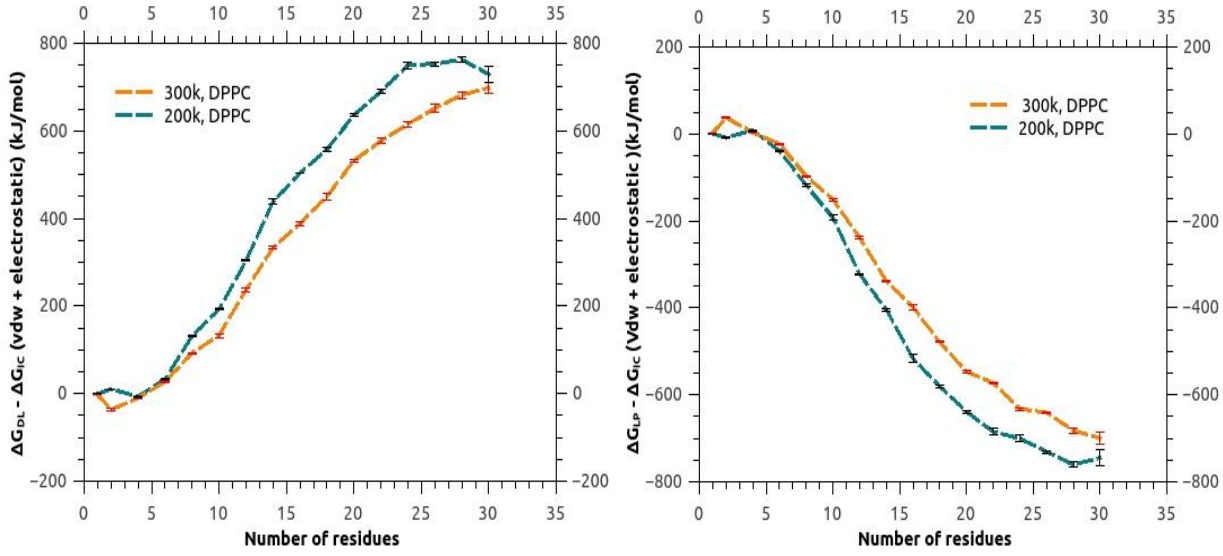

(A) **(B)**

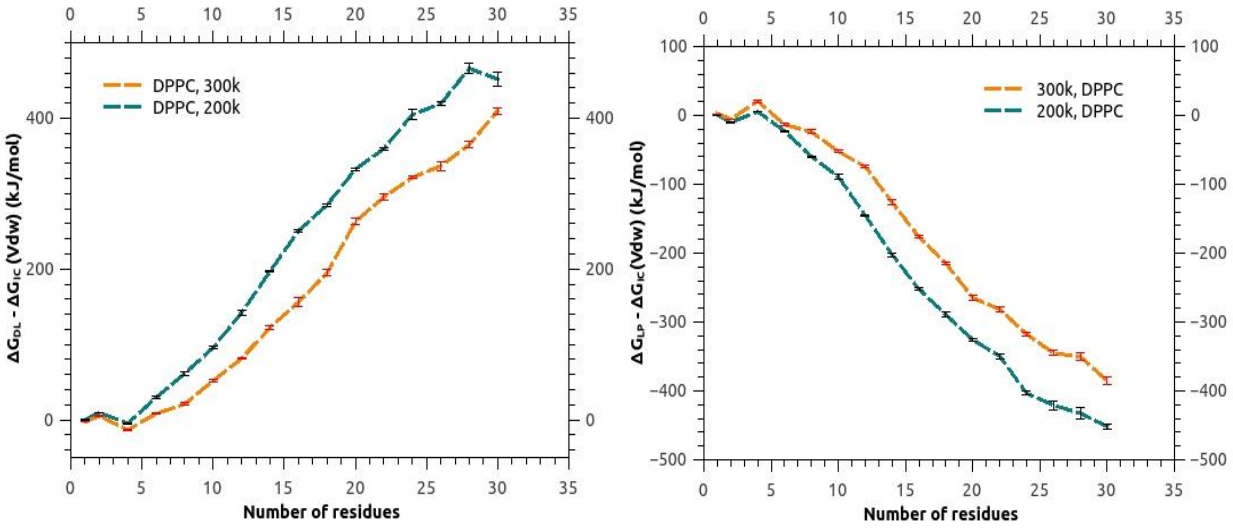

(C) **(D)**

Figure 8 : *variation in ΔG_{DL} - ΔG_{IC} **(A)** Including both electrostatic (q) and van der Waals (Vdw) interactions **(C)** Including only van der Waals (Vdw) interactions. Variation in ΔG_{LP} - ΔG_{IC} **(B)** Including both electrostatic (q) and van der Waals (Vdw) interactions **(D)** including only van der Waals (Vdw) interactions, with number of residues of mixed bead type polyalanine in kJ/mol, at 300k and 200k with DPPC bilayer.*

A similar minor kink is also observed at ALA_26 as an indication of membrane core/acyl chain region. This suggests that temperature reduction have positive increase the values of free energy of delipidation and lipidation.

Lipophobic contributions

Values of ΔG_{DLLC} - ΔG_{IC} and ΔG_{LPLC} - ΔG_{IC} were found to be nearly similar as 300 K until ALA_6. ALA_8 and ALA_10 have higher values of ΔG_{DLLC} - ΔG_{IC} and ΔG_{LPLC} - ΔG_{IC} compared to 300 K. As discussed previously, ALA_12 onwards apolar beads are introduced to the structure. Again, this can be the possible reason that this values at higher values of ΔG_{DLLC} - ΔG_{IC} and ΔG_{LPLC} - ΔG_{IC} at 200k. A slight discrepancy was observed in the values of delipidation and lipidation at ALA_12, ALA_28 and ALA_30 (Fig.9 (A) and (B)). Increment or decay observed in the values was neither additive nor constant in nature (Spp. Table 10).

On the other hand, individual contribution from van der Waals interactions tend to have elevated values at 200 K expect ALA_1 and ALA_2, which have nearly identical values of contributions. A minor kink, which is observed in previous results as well, remains consistent will these results. However, a minor discrepancy between the values ΔG_{DLLC} - ΔG_{IC} and ΔG_{LPLC} - ΔG_{IC} is seen around ALA_22 (Fig.9 (C) and (D)). Values for contributions from van der Waals interactions also have clear trend in terms of increment (Spp. Table 11).

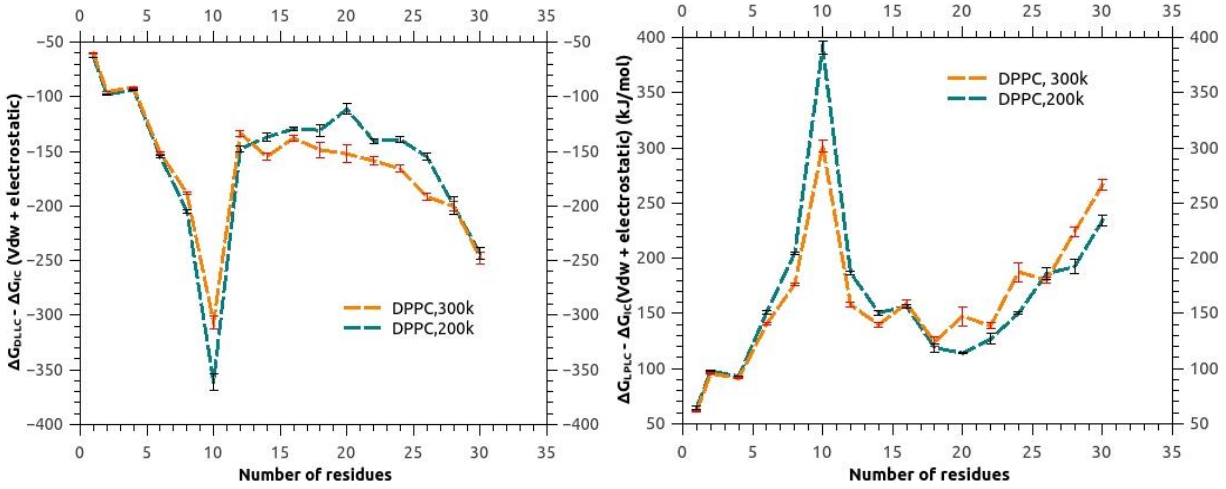

(A) **(B)**

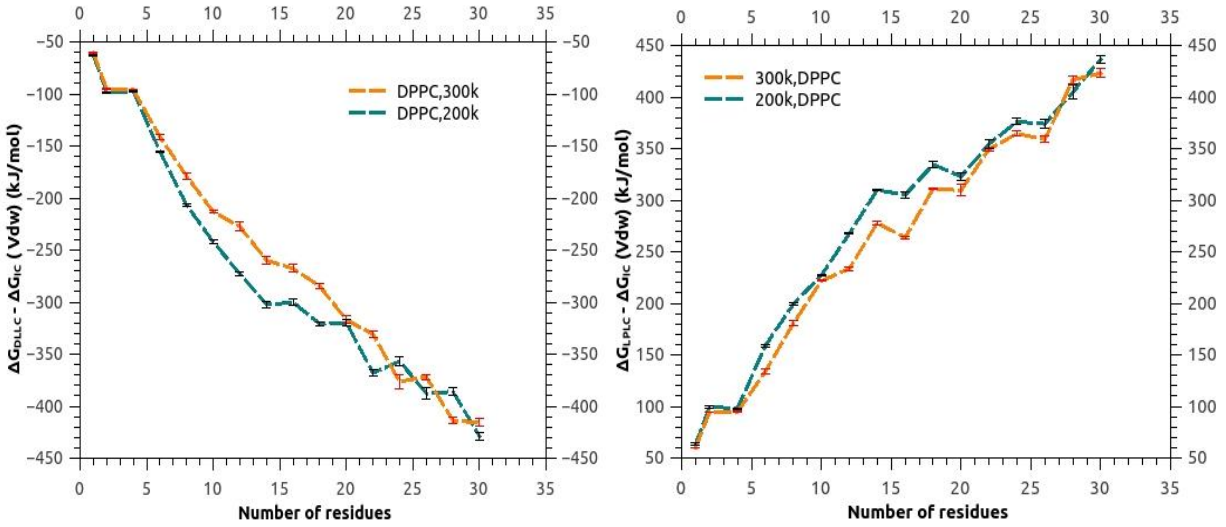

(C) **(D)**

Figure 9: *variation in ΔG_{DLLC} - ΔG_{IC} **(A)** Including both electrostatic (q) and van der Waals (Vdw) interactions **(C)** Including only van der Waals (Vdw) interactions. Variation in ΔG_{LPLC} - ΔG_{IC} **(B)** Including both electrostatic (q) and van der Waals (Vdw) interactions **(D)** including only van der Waals (Vdw) interactions, with number of residues of mixed bead type polyalanine in kJ/mol, at 300k and 200k with DPPC bilayer.*

Energetics of Polyalanine peptides in DOPC bilayers

Values of ΔG_{DL} - ΔG_{IC} and ΔG_{LP} - ΔG_{IC} are found to be increasing with a higher rate in the case of DOPC bilayer compared to DPPC bilayer at 300k until the transition from ALA_14 to ALA_16. Interestingly, at the same point values ΔG_{DL} - ΔG_{IC} and ΔG_{LP} - ΔG_{IC} values of become lesser in the case DOPC bilayer. Although, values continue to rise until ALA_26, where a kink is observed as an indication of head group region.

Fig. 10(C) and (D) shows the variation in energetics associated with van der Waals interactions between peptide and lipid environment. Similar to the previous case, values of energetics tend to rise with higher rate compared to DPPC bilayer initially, but ALA_12 onwards increment rate of values decays. ALA_20 onwards values become nearly identical for both DPPC and DOPC bilayer.

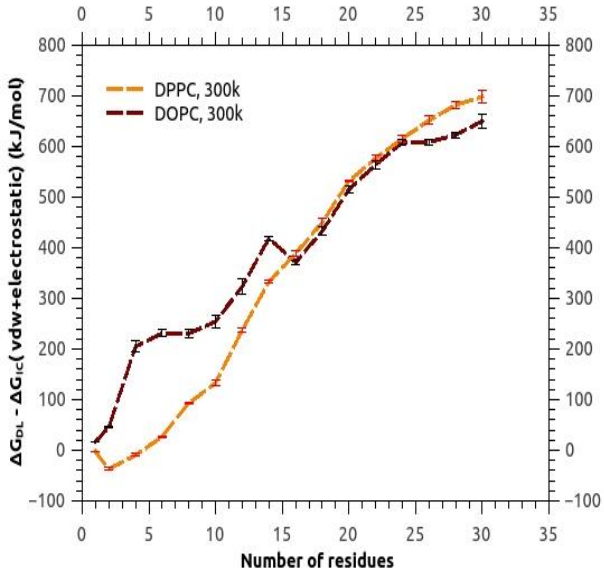

(A)

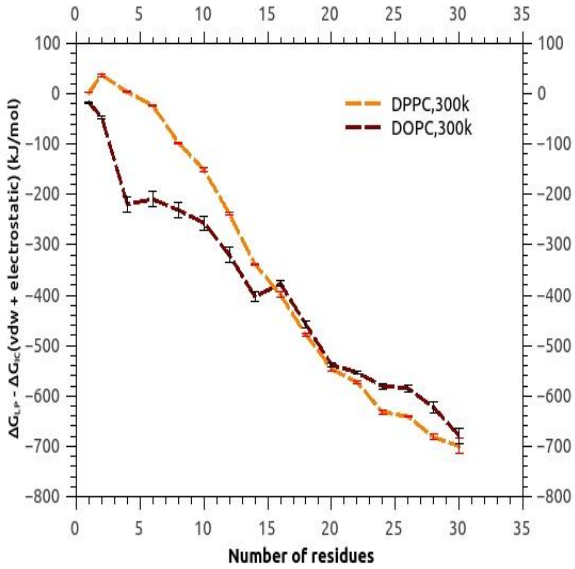

(B)

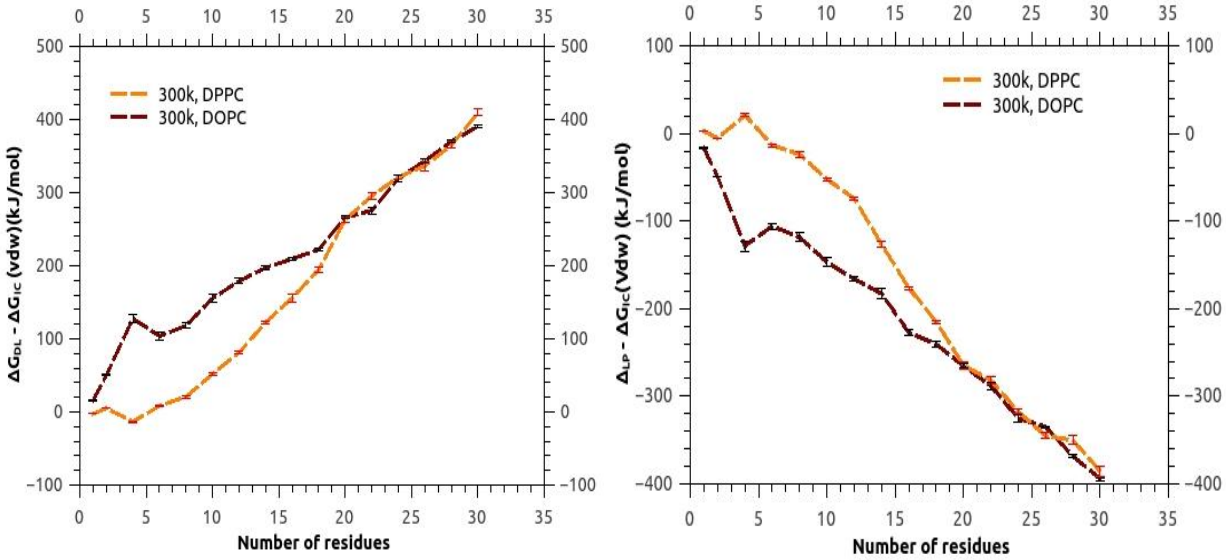

(C) **(D)**

Figure 10: *variation in ΔG_{DL} - ΔG_{IC} (**A)** Including both electrostatic (q) and van der Waals (Vdw) interactions (**C)** Including only van der Waals (Vdw) interactions. Variation in ΔG_{LP} - ΔG_{IC} (**B)** Including both electrostatic (q) and van der Waals (Vdw) interactions **(D)** including only van der Waals (Vdw) interactions, with number of residues of mixed bead type polyalanine in kJ/mol, at 300k with DPPC and DOPC bilayer.*

Critical observation of Fig. 10 (A), (B), (C) and (D) suggests that increment rate of energetics in not uniform. Values increase higher rate for more polar structures, but as apolar beads are added at the center of peptide successively, hydrophobicity of the peptide increases and the values of energetics tend to increase with a slower rate. Graph for ΔG_{DL} - ΔG_{IC} and ΔG_{LP} - ΔG_{IC} in both cases are found symmetrical. This ensures reversibility of our energetics in the case DOPC bilayer (Spp. Table 12 & 13).

Lipophobic contributions

Interestingly, values of ΔG_{DLLC} - ΔG_{IC} and ΔG_{LPLC} - ΔG_{IC} in the case of DOPC bilayer to be opposite in sign as observed in the case of DPPC. This indicates that less ordered DOPC bilayer tend to interact better with a peptide and supports the solvation of the peptide. Values of ΔG_{DLLC} - ΔG_{IC} and ΔG_{LPLC} - ΔG_{IC} clearly imply that cost of cavity formation for lipidation and delipidation is negative and positive respectively. This concludes that cavity

formation for the insertion of mixed bead type polyalanine is favorable and will be spontaneous. However, increment in the values is not uniform. Values decrease as we move to ALA_1 to ALA_2 the values increase sharply until ALA_6. In the case of ALA_8 and ALA_10 there is not much change observed in the values. At ALA_12, there is a drastic increment observed but after that values remain almost constant until ALA_26, where an extremely slow decay is observed possibly as an indication of acyl chain region (Fig. 11(A) and (B)). DOPC bilayer, which is more fluid in nature compared to DPPC bilayer, is expected to show such results, since due to its less ordered structure, its lipids tails are freer to interact with peptide. Hence, favors the insertion of the peptide inside a bilayer. Fig. 11(C) and (D) shows the variations individual variation of van der Waals interactions involved in lipophobic contributions in the case DOPC and DPPC bilayer. Signs of the values of remain consistent with previous results observed in the case of Fig. 11(A) and (B). This denotes that van der Waals interactions also supports the lipidation of peptide in the bilayer and cavity formation will be spontaneous. Although, Increments observed in van der Wall interactions are not uniform. Values decrease from ALA_1 and ALA_2 and then doesn't vary much for ALA_4. This is followed a sharp increase at ALA_6. Interestingly, ALA_6 onwards, values remain nearly constant for rest of residues. Graphs for both delipidation are found to be symmetrical. This ensured the reversibly of lipophobic contributions in the case of DOPC bilayer (Spp. Table 14 & 15).

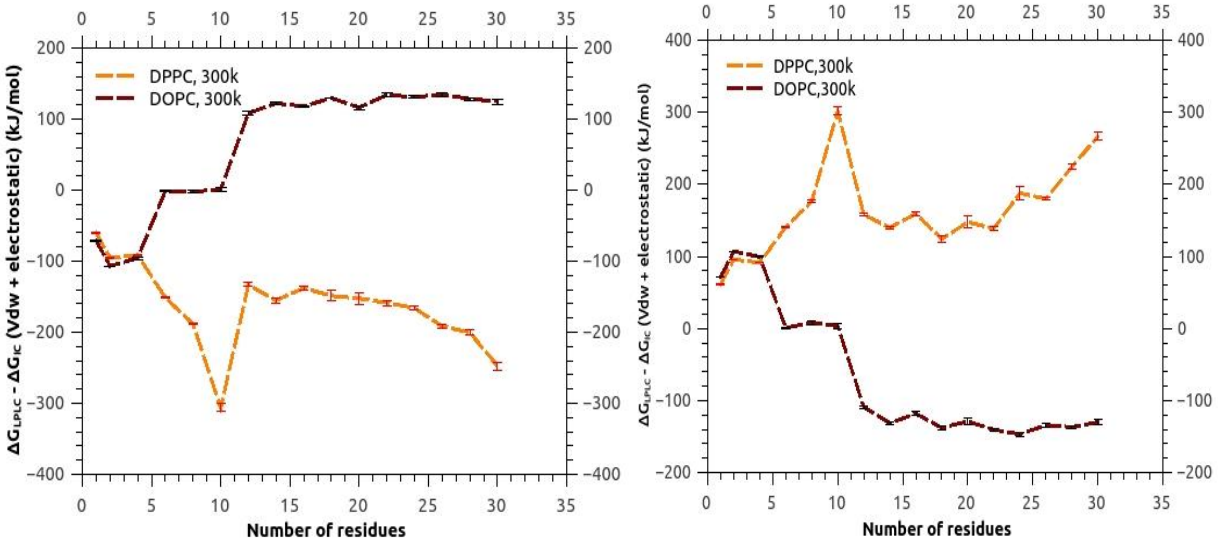

(A) **(B)**

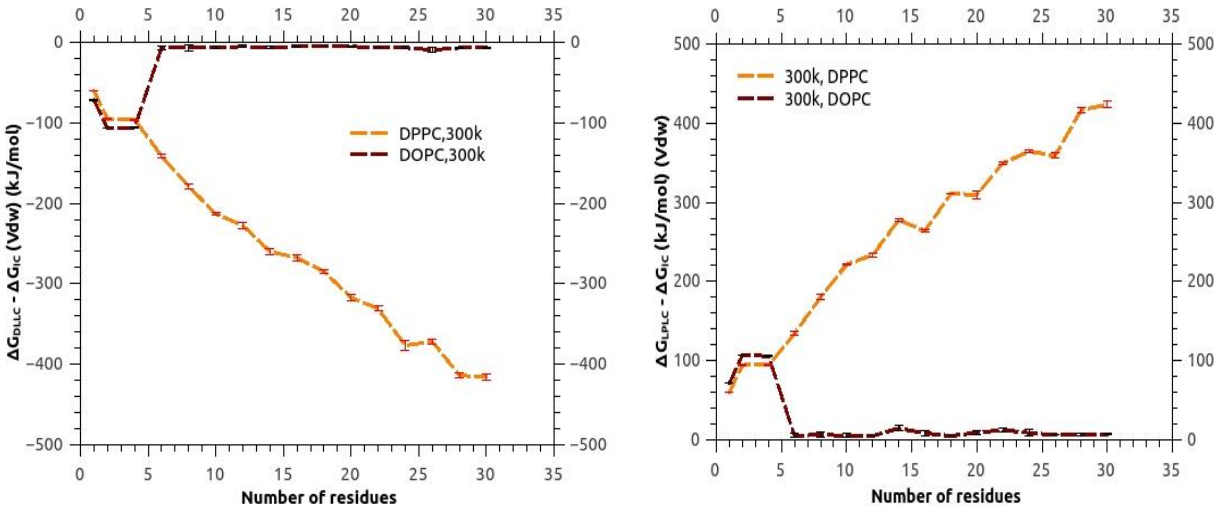

(C) **(D)**

Figure 11: *variation in ΔG_{DLLC} - ΔG_{IC}* ***(A)*** *Including both electrostatic (q) and van der Waals (Vdw) interactions* ***(C)*** *Including only van der Waals (Vdw) interactions. Variation in ΔG_{LPLC} - ΔG_{IC}* ***(B)*** *Including both electrostatic (q) and van der Waals (Vdw) interactions* ***(D)*** *including only van der Waals (Vdw) interactions, with number of residues of mixed bead type polyalanine in kJ/mol, at 300k with DPPC and DOPC bilayer.*

Conclusion

In this work, we have studied the energetics of the membrane insertion of different peptide moieties and polyalanine peptides of varying length. As our primary objective, we have estimated the energetics of lipophobic contribution i.e. for the cost of cavity formation involved in delipidation and lipidation and presented detailed quantitative values for all 39 bead subtypes and polyalanine peptides of varying lengths. Additionally, we have calculated the free energy of lipidation and delipidation of individual bead-types and polyalanine peptides and compared to previous experimental and simulation data, where possible. We have been successful in decomposing the individual contribution of van der Waals interactions present between peptide and lipids.

Interestingly, our study suggests that the lipophobic contribution is substantial. Or results are a clear indication that protein-protein is not the only factor which drive transmembrane protein insertion and association but protein-lipid interactions are also possibly play a

critical role in these processes. Results obtained by varying the temperature indicates that free energy of delipidation/lipidation and lipophobic contributions tend to increase as the temperature is lowered. Lipophobic contribution for polyalanine with less ordered DOPC bilayer found to be negative i.e. cavity formation is became favorable for polyalanine insertion, when switched to DOPC bilayer. Since both of these parameters affect membrane fluidity, we can conclude that membrane fluidity affects both, free energy of delipidation/lipidation and lipophobic contributions.

Overall, our study brings a new prospective to look at membrane protein interactions, which is neglected for quite long. Obviously, it's a very broad and complex field to study and still a lot of effort is required to completely understand the in the study of membrane protein insertion and associations. However, our studies imparts a new factor to researchers working in this field and provides enough evidence to encourage them to work in this direction. Hopefully, our study will turned out to be an important milestone in this journey to understand membrane protein interactions and cellular membrane.

References

[1] A. Rath and Charles M. Deber. Protein structure in membrane domains. *Annu. Rev. Biophys*., **2012,** 41:135–155.

[2] C. Finger, C. Escher, and Schneider. The single transmembrane domains of human receptor tyrosine kinases encode self-interactions. *Science Signaling, **2009,** 2(89): ra56*.

[3] J. B. Casaletto and A. I. McClatchey. Spatial regulation of receptor tyrosine kinases in development and cancer. *Nat Rev Cancer, **2012,** 12(6): ra56*.

[4] David Chandler. Interfaces and the driving force of hydrophobic assembly. *Nature, **2005,** 437(7059):640–647.*

[5] F Jähnig. Thermodynamics and kinetics of protein incorporation into membranes. *Proc. Natl. Acad. Sci. U. S. A., **1983**, 80(12):3691–3695.*

[6] Shachi Katira, Kranthi K. Mandadapu, Suriyanarayanan Vaikuntanathan, Berend Smit, David Chandler. The order-disorder phase transition in lipid bilayers mediates a force for assembly of transmembrane proteins. *arXiv: 1506.04298 [cond-mat.soft], **2015**.*

[7] Aiswarya B. Pawar, Sneha A. Deshpande, Srinivasa M. Gopal, Tsjerk A. Wassenaar, Chaitanya A. Athale, and Durba Sengupta. Thermodynamic and kinetic characterization of transmembrane helix association. *Phys. Chem. Chem. Phys., **2015**, 17:1390–1398.*

[8] Siewert J. Marrink, H. Jelger Risselada, Serge Yefimov, D. Peter Tieleman, and Alex H.de Vries. The *MARTINI* force field: Coarse-grain model for biomolecular simulations. *J. Phys. Chem. B, **2007**, 111(27):7812–7824.*

[9] David Van Der Spoel, Erik Lindahl, Berk Hess, Gerrit Groenhof, Alan E. Mark, and Herman J. C. Berendsen. *GROMACS:* Fast, flexible, and free. *J Comput Chem, **2005**, 26(16):1701–1718.*

[10] Berendsen H. J. C., J. P. M. Postma, W. F. van Gunsteren, A. DiNola, and J. R. Haak. Molecular-dynamics with coupling to an external bath. *J Chem. Phys. **1984**, 81(8):3684–3690.*

[11] Timir Hajari and Nico F. A. van der Vegt. Solvation thermodynamics of amino acid side chains on a short peptide backbone. *J. Chem. Phys. **2015**, 142(14).*

[12] J. G. Kirkwood. Statistical mechanics of fluid mixtures, J. Chem. Phys. , **1935**, 3:300-313.

[13] Frenkel, Daan and Smit, Berend. Understanding Molecular Simulation: From Algorithms to Applications. Academic Press, ***2007***

[14] Andrew R. Leach, Molecular Modelling: Principles and Applications, ***ISBN-13: 978-0582382107, Pearson; 2 edition***

[15] Siewert J. Marrink, Alex H. de Vries, and Alan E. Mark. Coarse-Grained Model for Semiquantitative Lipid Simulations*, J. Phys. Chem. B. **2004**, 108, 750-760*

[16] Alder, B.J.; T. E. Wainwright, Studies in Molecular Dynamics. I. General Method*, **1959**, J. Chem. Phys. 31 (2).*

[17] A. Rahman Correlations in the Motion of Atoms in Liquid Argon, ***1964**, Phys Rev 136 (2A).*

[18] Martin Karplus and Gregory A. Petsko, Molecular Dynamics Simulations in Biology*, Nature **1990**,Vol. 347,*

[19] Stewart A. Adcock and J. Andrew McCammon, Molecular Dynamics: Survey of Methods for Simulating the Activity of Proteins, *Chem. Rev. **2006**, 106, 1589-1615*

[20] Olaf S. Andersen and Roger E. Koeppe, Bilayer Thickness and Membrane Protein Function: An Energetic Perspective*, Annu. Rev. Biophys. Biomol. Struct. **2007**. 36:107–130*

[21] Alessandra Villa, Alan E. Mark, Calculation of the Free Energy of Solvation for Neutral Analogs of Amino Acid Side Chains, *J Comput Chem, **2002**, 23: 548–553,*

[22] Chipot, C.; Pohorille, A. *Free Energy Calculations – Theory and Applications in Chemistry and Biology; Springer: Berlin,* ***2007***

[23] Miguel Jorge, Nuno M. Garrido, Antonio J. Queimada, Ioannis G. Economou, and Eugenia A. Macedo , Effect of the Integration Method on the Accuracy and Computational Efficiency of Free Energy Calculations Using Thermodynamic Integration*, J. Chem. Theory Comput.,* ***2010*** *6(4),*

Supplementary data

Bead type	ΔG_{DL}	ΔG_{LP}	ΔG_{DLLC}	ΔG_{LPLC}
Qd	**-45.49 ± 0.45**	**47.84 ± 1.07**	**-136.70 ± 2.05**	**135.19 ± 1.42**
Qa	**-44.91 ± 0.34**	**45.41 ± 0.44**	**-134.41 ± 2.66**	**134.87 ± 1.06**
Q0	**-47.86 ± 1.20**	**43.37 ± 0.25**	**-141.97 ± 1.00**	**134.96 ± 1.35**
Qda	**-47.80 ± 0.50**	**45.06 ± 0.60**	**-134.18 ± 0.78**	**135.58 ± 2.08**
P5	**-3.75 ± 0.23**	**3.15 ± 0.17**	**-60.98 ± 0.15**	**60.82 ± 0.19**
P4	**-2.67 ± 0.12**	**2.68 ± 0.10**	**-60.34 ± 0.13**	**61.31 ± 0.28**
P3	**-1.32 ± 0.18**	**0.94 ± 0.13**	**-53.59 ± 1.11**	**60.25 ± 0.67**
P2	**-1.95 ± 0.10**	**1.64 ± 0.12**	**-55.59 ± 1.35**	**59.56 ± 0.38**
P1	**2.36 ± 0.17**	**-2.86 ± 0.09**	**-54.42 ± 0.73**	**62.29 ± 0.70**
Nd	**1.65 ± 0.21**	**-2.32 ± 0.15**	**-57.68 ± 0.84**	**57.88 ± 1.37**
Na	**1.87 ± 0.11**	**-2.04 ± 0.04**	**-55.84 ± 1.33**	**55.18 ± 0.55**
N0	**1.31 ± 0.17**	**-1.33 ± 0.17**	**-61.36 ± 0.67**	**58.59 ± 1.34**
Nda	**2.26 ± 0.15**	**-2.35 ± 0.18**	**-60.30 ± 0.92**	**63.37 ± 0.76**

C5	**4.81 ± 0.31**	**-5.34 ± 0.06**	**-59.60 ± 0.80**	**62.41 ± 0.12**
C4	**4.41 ± 0.08**	**-4.51 ± 0.16**	**-58.49 ± 0.90**	**59.30 ± 1.19**
C3	**8.99 ± 0.12**	**-9.28 ± 0.08**	**-65.26 ± 1.78**	**59.03 ± 0.48**
C2	**10.32 ± 0.15**	**-10.64 ± 0.08**	**-62.88 ± 0.85**	**67.87 ± 0.57**
C1	**10.42 ± 0.11**	**-10.24 ± 0.08**	**-65.02 ± 0.71**	**66.19 ± 1.60**
SQd	**-44.27 ± 0.60**	**45.81 ± 1.06**	**0.00 ± 0.00**	**0.00 ± 0.00**
SQa	**-48.05 ± 0.81**	**45.33 ± 0.41**	**0.00 ± 0.00**	**0.00 ± 0.00**
SQ0	**-45.13 ± 1.17**	**43.55 ± 1.02**	**0.00 ± 0.00**	**0.00 ± 0.00**
SQda	**-45.13 ± 1.17**	**44.77 ± 0.70**	**0.00 ± 0.00**	**0.00 ± 0.00**
SP5	**-3.06 ± 0.06**	**3.13 ± 0.10**	**-61.22 ± 0.26**	**60.83 ± 0.22**
SP4	**-3.70 ± 0.17**	**4.08 ± 0.04**	**-51.44 ± 0.98**	**53.89 ± 1.14**
SP3	**-0.77 ± 0.14**	**0.67 ± 0.06**	**-55.29 ± 0.87**	**56.23 ± 0.79**
SP2	**-1.72 ± 0.08**	**1.64 ± 0.18**	**-58.93 ± 0.82**	**54.77 ± 0.93**
SP1	**3.03 ± 0.12**	**-1.90 ± 0.37**	**-56.58 ± 1.99**	**59.83 ± 0.64**
SNd	**1.70 ± 0.25**	**-2.14 ± 0.10**	**-58.20 ± 0.29**	**56.60 ± 0.65**
SNa	**2.06 ± 0.09**	**-1.73 ± 0.14**	**-58.03 ± 1.50**	**57.23 ± 0.63**
SN0	**1.00 ± 0.17**	**-1.00 ± 0.14**	**-61.41 ± 0.29**	**59.60 ± 0.98**
SNda	**2.44 ± 0.07**	**-1.73 ± 0.15**	**-60.56 ± 0.93**	**55.69 ± 1.30**
SC5	**5.37 ± 0.16**	**-5.25 ± 0.20**	**-61.09 ± 1.26**	**61.23 ± 1.07**
SC4	**4.51 ± 0.08**	**-4.48 ± 0.13**	**-60.51 ± 0.70**	**59.63 ± 0.83**
SC3	**9.10 ± 0.07**	**-9.20 ± 0.15**	**-62.28 ± 1.61**	**62.44 ± 1.94**

SC2	**9.10 ± 0.07**	**-10.67 ± 0.15**	**-66.95 ± 0.34**	**62.28 ± 0.89**
SC1	**9.39 ± 0.32**	**-10.20 ± 0.13**	**0.00 ± 0.00**	**0.00 ± 0.00**
AC1	**8.02 ± 0.17**	**-7.93 ± 0.13**	**-63.96 ± 1.18**	**67.67 ± 0.88**
AC2	**8.37 ± 0.11**	**-7.99 ± 0.35**	**-62.09 ± 0.88**	**66.77 ± 1.14**
BP4	**9.95 ± 0.05**	**-9.81 ± 0.04**	**-54.84 ± 1.00**	**53.68 ± 0.28**

***Spp. Table 1**: ΔG_{DL}, ΔG_{LP}, ΔG_{DLLC} and ΔG_{LPLC} for all bead types of MARTINI forcefield in kJ/mol, at 300k with DPPC bilayer*

Residues	ΔG_{DL}	ΔG_{LP}	$\Delta G_{DL} - \Delta G_{IC}$	$\Delta G_{LP} - \Delta G_{IC}$
1	**5.36 ± 0.11**	**-4.66 ± 0.24**	**5.36 ± 0.11**	**-4.66 ± 0.24**
2	**19.75 ± 0.27**	**-19.80 ± 0.33**	**20.08 ± 0.20**	**-20.18 ± 0.09**
4	**50.88 ± 0.27**	**-51.66 ± 0.43**	**46.10 ± 0.18**	**-46.26 ± 0.18**
6	**83.58 ± 0.45**	**-83.61 ± 0.59**	**70.50 ± 0.36**	**-71.35 ± 0.85**
8	**115.44 ± 1.16**	**-113.14 ± 0.83**	**93.70 ± 0.96**	**-96.13 ± 0.46**
10	**144.69 ± 1.13**	**-147.48 ± 0.58**	**116.39 ± 1.11**	**-119.18 ± 0.56**
12	**178.02 ± 1.14**	**-178.40 ± 1.59**	**139.24 ± 1.57**	**-142.34 ± 1.56**
14	**212.44 ± 0.95**	**-208.31 ± 1.04**	**164.27 ± 1.78**	**-166.04 ± 1.71**
16	**244.53 ± 1.65**	**-243.37 ± 0.30**	**189.78 ± 2.02**	**-191.63 ± 0.24**
18	**282.53 ± 1.82**	**-273.95 ± 1.53**	**222.78 ± 1.39**	**-214.35 ± 1.45**
20	**315.62 ± 1.12**	**-315.62 ± 2.07**	**245.24 ± 3.61**	**-248.11 ± 1.97**
22	**349.22 ± 4.95**	**-345.64 ± 1.61**	**273.82 ± 5.06**	**-270.24 ± 1.72**

24	**371.15 ± 2.10**	**-370.89 ± 2.63**	**287.80 ± 2.24**	**-287.54 ± 2.77**
26	**378.21 ± 8.65**	**-380.89 ± 2.63**	**286.92 ± 8.83**	**-289.26 ± 8.36**
28	**418.97 ± 1.23**	**-425.27 ± 5.37**	**319.71 ± 1.44**	**-326.01 ± 5.58**
30	**453.87 +/ - 5.59**	**-455.87 ± 4.32**	**346.61 ± 5.83**	**-348.61 ± 4.56**

Spp. Table 2*: ΔG_{DL}, ΔG_{LP}, $\Delta G_{DL} - \Delta G_{IC}$ and $\Delta G_{LP} - \Delta G_{IC}$ for different lengths of single bead type polyalanine (C5 bead only) in kJ/mol, at 300k with DPPC bilayer.*

Residues	ΔG_{DL}	ΔG_{LP}	$\Delta G_{DL} - \Delta G_{IC}$	$\Delta G_{LP} - \Delta G_{IC}$
1	**-64.53 ± 0.71**	**58.10 ± 1.40**	**-64.53 ± 0.71**	**58.10 ± 1.40**
2	**-96.71 ± 1.01**	**91.57 ± 1.53**	**-96.71 ± 1.01**	**91.57 ± 1.53**
4	**-138.49 ± 0.84**	**139.21 ± 2.78**	**-143.09 ± 0.84**	**143.81 ± 2.78**
6	**-180.66 ± 1.22**	**160.45 ± 4.32**	**-192.73 ± 1.23**	**172.52 ± 4.33**
8	**-193.21 ± 2.02**	**197.05 ± 1.71**	**-213.60 ± 2.04**	**217.44 ± 1.73**
10	**-226.40 ± 2.18**	**214.30 ± 1.72**	**-254.70 ± 2.21**	**242.60 ± 1.75**
12	**-238.42 ± 2.00**	**232.65 ± 0.87**	**-274.50 ± 2.03**	**268.73 ± 0.90**
14	**-239.28 ± 2.81**	**244.39 ± 2.07**	**-283.18 ± 2.85**	**288.29 ± 2.11**
16	**-250.50 ± 2.22**	**244.09 ± 1.40**	**-302.25 ± 2.29**	**295.84 ± 1.47**
18	**-266.28 ± 3.60**	**247.67 ± 2.34**	**-325.90 ± 3.68**	**307.29 ± 2.42**
20	**-277.12 ± 6.65**	**268.27 ± 2.48**	**-344.63 ± 6.75**	**335.78 ± 2.58**
22	**-283.51 ± 3.54**	**269.61 ± 1.88**	**-358.93 ± 3.66**	**345.03 ± 2.00**
24	**-294.94 ± 1.46**	**306.57 ± 5.85**	**-378.27 ± 1.60**	**389.90 ± 5.99**

26	**-311.00 ± 6.54**	**306.91 ± 6.11**	**-402.30 ± 6.71**	**398.21 ± 6.28**
28	**-337.15 ± 6.99**	**335.46 ± 9.06**	**-436.38 ± 7.20**	**434.69 ± 9.27**
30	**-328.34 ± 3.53**	**322.30 ± 3.04**	**-435.58 ± 3.77**	**429.54 ± 3.28**

***Spp. Table 3**: ΔG_{DLLC}, ΔG_{LPLC}, ΔG_{DLLC} - ΔG_{IC} and ΔG_{LPLC} - ΔG_{IC} for different lengths of single bead type polyalanine (C5 bead only) in kJ/mol, at 300k with DPPC bilayer.*

Residues	ΔG_{DL}	ΔG_{LP}	ΔG_{DL} - ΔG_{IC}	ΔG_{LP} - ΔG_{IC}
1	**-2.67 ± 0.12**	**2.53 ± 0.11**	**-2.67 ± 0.12**	**2.53 ± 0.11**
2	**-33.59 ± 0.23**	**34.08 ± 0.49**	**-36.83 ± 2.22**	**37.32 ± 2.48**
4	**98.06 ± 2.75**	**-104.25 ± 1.31**	**-9.68 ± 2.76**	**3.49 ± 1.32**
6	**144.06 ± 1.08**	**-140.57 ± 0.84**	**26.85 ± 1.09**	**-23.36 ± 0.85**
8	**127.60 ± 1.26**	**-131.83 ± 1.27**	**92.92 ± 1.31**	**-97.15 ± 1.32**
10	**201.37 ± 4.42**	**-218.97 ± 3.09**	**133.03 ± 4.43**	**-150.63 ± 3.10**
12	**273.33 ± 4.10**	**-274.43 ± 3.14**	**237.54 ± 4.13**	**-238.64 ± 3.17**
14	**376.68 ± 2.56**	**-381.86 ± 0.76**	**333.06 ± 2.61**	**-338.24 ± 0.81**
16	**440.01 ± 5.39**	**-450.42 ± 4.84**	**388.56 ± 5.45**	**-398.97 ± 4.90**
18	**509.72 ± 7.99**	**-538.02 ± 1.75**	**450.40 ± 8.07**	**-478.70 ± 1.83**
20	**599.37 ± 2.33**	**-613.67 ± 3.97**	**532.15 ± 2.42**	**-546.45 ± 4.06**
22	**651.79 ± 6.27**	**-648.02 ± 2.56**	**576.68 ± 6.38**	**-572.91 ± 2.67**
24	**698.45 ± 5.79**	**-715.34 ± 3.15**	**615.42 ± 5.94**	**-632.31 ± 3.30**
26	**742.61 ± 7.9**	**-732.01 ± 2.06**	**651.62 ± 8.08**	**-641.02 ± 2.24**

28	**781.56 ± 7.35**	**-781.54 ± 4.9**	**681.99 ± 8.21**	**-681.97 ± 5.76**
30	**812.93 ± 4.59**	**-814.26 ± 6.61**	**698.43 ± 13.11**	**-699.76 ± 15.13**

Spp. Table 4*: ΔG_{DL}, ΔG_{LP}, ΔG_{DL} - ΔG_{IC} and ΔG_{LP} - ΔG_{IC} for different lengths of mixed bead type polyalanine including both electrostatic (q) and van der Waals (Vdw) interactions in kJ/mol, at 300k with DPPC bilayer.*

Residues	ΔG_{DL}	ΔG_{LP}	ΔG_{DL} - ΔG_{IC}	ΔG_{LP} - ΔG_{IC}
1	**-2.55 ± 0.09**	**2.53 ± 0.11**	**-2.55 ± 0.09**	**2.53 ± 0.11**
2	**5.09 ± 0.16**	**-5.51 ± 0.13**	**5.09 ± 0.16**	**-5.51 ± 0.13**
4	**-5.24 ± 0.94**	**12.64 ± 1.57**	**-13.39 ± 0.95**	**20.79 ± 1.57**
6	**21.30 ± 1.08**	**-26.63 ± 1.82**	**8.17 ± 1.09**	**-13.51 ± 1.83**
8	**41.25 ± 1.85**	**-44.35 ± 2.79**	**20.86 ± 1.87**	**-23.95 ± 2.81**
10	**80.09 ± 1.27**	**-80.68 ± 2.03**	**51.76 ± 1.29**	**-52.33 ± 2.06**
12	**116.98 ± 3.24**	**-110.18 ± 1.53**	**81.20 ± 1.29**	**-74.39 ± 1.57**
14	**166.06 ± 2.44**	**-170.01 ± 3.48**	**122.46 ± 2.48**	**-126.42 ± 3.52**
16	**207.56 ± 5.64**	**-227.76 ± 1.87**	**156.1 ± 5.70**	**-176.3 ± 1.93**
18	**253.81 ± 4.13**	**-274.34 ± 1.25**	**194.48 ± 4.21**	**-215.02 ± 1.33**
20	**330.10 ± 3.80**	**-332.03 ± 4.00**	**262.9 ± 3.9**	**-264.81 ± 4.10**
22	**370.43 ± 4.83**	**-356.69 ± 3.67**	**295.3 ± 4.94**	**-281.55 ± 3.78**
24	**404.25 ± 1.88**	**-400.54 ± 2.56**	**321.24 ± 2.02**	**-317.53 ± 2.70**
26	**427.56 ± 6.12**	**-436.11 ± 3.45**	**336.56 ± 6.29**	**-345.1 ± 3.62**

28	**463.78 ± 4.41**	**-449.12 ± 4.86**	**364.81 ± 4.61**	**-350.17 ± 5.06**
30	**516.84 ± 3.95**	**-492.65 ± 5.69**	**409.88 ± 4.19**	**-385.68 ± 5.91**

Spp. Table 5 : *ΔG_{DL}, ΔG_{LP}, ΔG_{DL} - ΔG_{IC} and ΔG_{LP} - ΔG_{IC} for different lengths of mixed bead type polyalanine including only van der Waals (Vdw) interactions in kJ/mol, at 300k with DPPC bilayer.*

Residues	ΔG_{DLLC}	ΔG_{LPLC}	ΔG_{DLLC} - ΔG_{IC}	ΔG_{LPLC} - ΔG_{IC}
1	**-60.34 ± 0.13**	**61.50 ± 0.40**	**-60.34 ± 0.13**	**61.50 ± 0.40**
2	**-95.38 ± 0.32**	**95.56 ± 0.39**	**-95.38 ± 0.32**	**95.56 ± 0.39**
4	**293.07 ± 0.29**	**-293.31 ± 0.42**	**-91.55 ± 0.31**	**91.31 ± 0.44**
6	**247.64 ± 1.06**	**-258.64 ± 0.96**	**-151.41 ± 1.08**	**140.41 ± 0.98**
8	**165.73 ± 0.90**	**-177.61 ± 1.44**	**-188.30 ± 0.94**	**176.42 ± 1.48**
10	**-30.91 ± 5.51**	**26.21 ± 5.16**	**-306.42 ± 5.57**	**301.72 ± 5.22**
12	**-125.17 ± 2.71**	**149.64 ± 2.28**	**-133.30 ± 2.72**	**157.77 ± 2.29**
14	**-153.31 ± 3.30**	**138.12 ± 2.15**	**-155.07 ± 3.31**	**139.88 ± 2.16**
16	**-129.36 ± 2.97**	**150.47 ± 2.97**	**-137.91 ± 2.99**	**159.02 ± 2.99**
18	**-132.43 ± 7.41**	**107.86 ± 4.15**	**-148.78 ± 7.44**	**124.21 ± 4.18**
20	**-128.16 ± 8.02**	**123.27 ± 8.65**	**-152.34 ± 8.06**	**147.45 ± 8.69**
22	**-126.58 ± 3.49**	**106.71 ± 2.83**	**-158.61 ± 3.53**	**138.74 ± 2.87**
24	**-126.12 ± 3.25**	**147.78 ± 8.59**	**-166.01 ± 3.30**	**187.67 ± 8.64**
26	**-143.89 ± 3.06**	**132.32 ± 2.39**	**-191.64 ± 3.13**	**180.07 ± 2.46**
28	**-144.50 ± 4.00**	**168.21 ± 3.77**	**-200.33 ± 4.26**	**224.04 ± 4.03**

30	**-174.36 ± 5.26**	**193.34 ± 5.09**	**-247.56 ± 39.36**	**266.54 ± 39.19**

Spp. Table 6 *: ΔG_{DLLC}, ΔG_{LPLC}, ΔG_{DLLC} - ΔG_{IC} and ΔG_{LPLC} - ΔG_{IC} for different lengths of mixed bead type polyalanine including both electrostatic (q) and van der Waals (Vdw) interactions in kJ/mol, at 300k with DPPC bilayer.*

Residues	ΔG_{DLLC}	ΔG_{LPLC}	ΔG_{DLLC} - ΔG_{IC}	ΔG_{LPLC} - ΔG_{IC}
1	**-60.52 ± 0.28**	**59.88 ± 0.14**	**-60.52 ± 0.28**	**59.88 ± 0.14**
2	**-95.29 ± 0.45**	**94.44 ± 0.17**	**-95.29 ± 0.45**	**94.44 ± 0.17**
4	**-95.95 ± 0.60**	**94.77 ± 0.34**	**-95.95 ± 0.60**	**94.77 ± 0.34**
6	**-140.89 ± 2.03**	**133.71 ± 2.46**	**-141.25 ± 2.03**	**134.07 ± 2.46**
8	**-171.37 ± 3.13**	**172.88 ± 2.69**	**-179.01 ± 3.14**	**180.52 ± 2.70**
10	**-197.85 ± 1.28**	**206.23 ± 0.64**	**-213.25 ± 1.29**	**221.63 ± 0.65**
12	**-219.30 ± 4.07**	**225.36 ± 2.11**	**-227.43 ± 4.08**	**233.49 ± 2.12**
14	**-258.13 ± 3.33**	**275.98 ± 1.63**	**-259.90 ± 3.35**	**277.75 ± 1.65**
16	**-259.20 ± 3.54**	**255.18 ± 1.48**	**-267.75 ± 3.56**	**263.73 ± 1.50**
18	**-268.33 ± 2.20**	**294.63 ± 0.75**	**-284.68 ± 2.22**	**310.98 ± 0.77**
20	**-292.92 ± 3.54**	**285.28 ± 5.42**	**-317.11 ± 3.57**	**309.47 ± 5.45**
22	**-298.81 ± 2.94**	**317.45 ± 2.29**	**-330.84 ± 2.98**	**349.48 ± 2.33**
24	**-336.58 ± 6.53**	**324.55 ± 2.23**	**-376.49 ± 6.59**	**364.46 ± 2.29**
26	**-323.98 ± 2.47**	**311.17 ± 3.03**	**-371.76 ± 2.53**	**358.95 ± 3.09**
28	**-358.08 ± 3.08**	**361.00 ± 3.30**	**-413.72 ± 3.17**	**416.64 ± 3.39**

30	**-352.28 ± 3.52**	**359.57 ± 4.07**	**-415.83 ± 3.61**	**423.12 ± 4.16**

***Spp. Table 7**: ΔG_{DLLC}, ΔG_{LPLC}, ΔG_{DLLC} - ΔG_{IC} and ΔG_{LPLC} - ΔG_{IC} for different lengths of mixed bead type polyalanine including only van der Waals (Vdw) interactions in kJ/mol, at 300k with DPPC bilayer.*

Residues	ΔG_{DL}	ΔG_{LP}	ΔG_{DL} - ΔG_{IC}	ΔG_{LP} - ΔG_{IC}
1	**0.13 ± 0.26**	**0.64 ± 0.10**	**0.13 ± 0.26**	**0.64 ± 0.10**
2	**10.43 ± 0.78**	**-8.35 ± 0.33**	**10.43 ± 0.78**	**-8.35 ± 0.33**
4	**105.02 ± 1.63**	**-103.55 ± 1.33**	**-6.86 ± 1.64**	**8.33 ± 1.34**
6	**155.78 ± 1.42**	**-160.99 ± 1.82**	**33.85 ± 1.44**	**-39.06 ± 1.84**
8	**175.32 ± 1.07**	**-162.27 ± 2.62**	**131.38 ± 1.17**	**-118.33 ± 2.72**
10	**271.40 ± 2.18**	**-271.35 ± 5.28**	**192.68 ± 2.23**	**-192.63 ± 5.33**
12	**342.91 ± 1.73**	**-362.37 ± 2.18**	**303.59 ± 1.77**	**-323.05 ± 2.22**
14	**485.75 ± 6.60**	**-451.92 ± 2.78**	**438.11 ± 6.65**	**-404.28 ± 2.83**
16	**559.87 ± 0.48**	**-573.14 ± 9.01**	**503.85 ± 0.55**	**-517.12 ± 9.08**
18	**621.59 ± 4.43**	**-644.97 ± 2.70**	**557.20 ± 4.52**	**-580.58 ± 2.79**
20	**708.96 ± 2.23**	**-711.68 ± 3.47**	**636.17 ± 2.34**	**-638.89 ± 3.58**
22	**771.04 ± 3.96**	**-766.15 ± 6.69**	**689.82 ± 4.09**	**-684.93 ± 6.82**
24	**839.88 ± 7.85**	**-790.06 ± 6.80**	**750.24 ± 8.01**	**-700.42 ± 6.96**
26	**851.13 ± 3.97**	**-828.91 ± 2.68**	**753.05 ± 4.16**	**-730.83 ± 2.87**
28	**871.07 ± 3.08**	**-869.03 ± 3.55**	**762.75 ± 5.82**	**-760.71 ± 6.29**

30	**854.48 ± 5.27**	**-864.01 ± 3.81**	**729.04 ± 17.98**	**-738.57 ± 16.52**

***Spp. Table 8**: ΔG_{DL}, ΔG_{LP}, ΔG_{DL} - ΔG_{IC} and ΔG_{LP} - ΔG_{IC} for different lengths of mixed bead type polyalanine including both electrostatic (q) and van der Waals (Vdw) interactions in kJ/mol, at 200k with DPPC bilayer.*

Residues	ΔG_{DL}	ΔG_{LP}	ΔG_{DL} - ΔG_{IC}	ΔG_{LP} - ΔG_{IC}
1	**-0.33 ± 0.41**	**0.63 ± 0.25**	**-0.33 ± 0.41**	**0.63 ± 0.25**
2	**9.66 ± 0.31**	**-10.01 ± 0.70**	**9.66 ± 0.31**	**-10.01 ± 0.70**
4	**4.31 ± 1.32**	**-3.56 ± 0.78**	**-4.72 ± 1.32**	**5.47 ± 0.78**
6	**45.08 ± 1.29**	**-38.30 ± 0.88**	**29.56 ± 1.30**	**-22.78 ± 0.89**
8	**84.17 ± 1.80**	**-82.95 ± 0.91**	**61.21 ± 1.82**	**-59.99 ± 0.93**
10	**127.22 ± 2.23**	**-120.50 ± 3.31**	**95.73 ± 2.26**	**-89.01 ± 3.34**
12	**181.41 ± 2.80**	**-184.59 ± 0.81**	**142.08 ± 2.84**	**-145.26 ± 0.85**
14	**244.56 ± 1.56**	**-249.92 ± 2.56**	**196.91 ± 1.61**	**-202.27 ± 2.61**
16	**306.58 ± 1.77**	**-308.32 ± 1.57**	**250.57 ± 1.84**	**-252.31 ± 1.64**
18	**349.18 ± 1.38**	**-353.88 ± 3.90**	**284.79 ± 1.47**	**-289.49 ± 3.99**
20	**405.13 ± 1.34**	**-398.72 ± 1.62**	**332.34 ± 1.45**	**-325.93 ± 1.73**
22	**440.70 ± 1.67**	**-430.78 ± 3.91**	**359.48 ± 1.80**	**-349.56 ± 4.04**
24	**494.22 ± 6.92**	**-493.08 ± 2.70**	**404.58 ± 7.07**	**-403.44 ± 2.85**
26	**517.36 ± 3.10**	**-518.75 ± 6.46**	**419.25 ± 3.29**	**-420.64 ± 6.65**
28	**572.50 ± 7.33**	**-539.13 ± 7.86**	**465.93 ± 7.54**	**-432.56 ± 8.07**

30	**566.66 ± 9.29**	**-566.72 ± 3.4**	**451.58 ± 9.55**	**-451.64 ± 3.66**

Spp. Table 9*: ΔG_{DL}, ΔG_{LP}, ΔG_{DL} - ΔG_{IC} and ΔG_{LP} - ΔG_{IC} for different lengths of mixed bead type polyalanine including only van der Waals (Vdw) interactions in kJ/mol, at 200k with DPPC bilayer.*

Residues	ΔG_{DLLC}	ΔG_{LPLC}	ΔG_{DLLC} - ΔG_{IC}	ΔG_{LPLC} - ΔG_{IC}
1	**-63.99 ± 0.45**	**64.82 ± 1.53**	**-63.99 ± 0.45**	**64.82 ± 1.53**
2	**-98.15 ± 0.48**	**97.80 ± 0.37**	**-98.15 ± 0.48**	**97.80 ± 0.37**
4	**294.53 ± 0.34**	**-294.87 ± 0.28**	**-93.43 ± 0.36**	**93.09 ± 0.30**
6	**248.98 ± 0.79**	**-252.62 ± 0.28**	**-154.74 ± 0.79**	**151.10 ± 1.38**
8	**156.67 ± 1.50**	**-156.89 ± 1.35**	**-204.82 ± 1.55**	**204.60 ± 1.40**
10	**-74.78 ± 7.03**	**104.77 ± 5.77**	**-361.11 ± 7.08**	**391.10 ± 5.82**
12	**-137.98 ± 2.33**	**147.64 ± 2.08**	**-147.76 ± 2.34**	**186.56 ± 1.86**
14	**-133.97 ± 3.96**	**146.05 ± 1.94**	**-136.98 ± 3.98**	**150.65 ± 2.10**
16	**-119.22 ± 1.69**	**100.34 ± 3.69**	**-129.52 ± 1.71**	**156.35 ± 1.96**
18	**-112.05 ± 5.44**	**100.34 ± 3.69**	**-130.66 ± 5.47**	**118.95 ± 3.72**
20	**-84.50 ± 4.85**	**87.09 ± 0.77**	**-111.46 ± 4.89**	**114.05 ± 0.81**
22	**-105.12 ± 2.11**	**91.46 ± 4.81**	**-140.43 ± 2.16**	**126.77 ± 4.86**
24	**-95.46 ± 2.76**	**106.66 ± 1.46**	**-139.14 ± 2.81**	**150.34 ± 1.51**
26	**-103.04 ± 3.40**	**133.99 ± 5.46**	**-155.09 ± 3.48**	**186.04 ± 5.54**
28	**-138.17 ± 6.13**	**130.82 ± 4.58**	**-199.74 ± 8.16**	**192.39 ± 6.61**
30	**-163.78 ± 5.58**	**154.48 ± 5.09**	**-243.68 ± 5.58**	**234.38 ± 5.09**

***Spp. Table 10**: ΔG_{DLLC}, ΔG_{LPLC}, ΔG_{DLLC} - ΔG_{IC} and ΔG_{LPLC} - ΔG_{IC} for different lengths of mixed bead type polyalanine including both electrostatic (q) and van der Waals (Vdw) interactions in kJ/mol, at 200k with DPPC bilayer.*

Residues	ΔG_{DLLC}	ΔG_{LPLC}	ΔG_{DLLC} - ΔG_{IC}	ΔG_{LPLC} - ΔG_{IC}
1	-63.19 ± 0.33	63.42 ± 0.86	-63.19 ± 0.33	63.42 ± 0.86
2	-98.47 ± 0.38	99.46 ± 0.93	-98.47 ± 0.38	99.46 ± 0.93
4	-97.43 ± 0.37	98.03 ± 0.58	-97.43 ± 0.37	98.03 ± 0.58
6	-154.78 ± 0.91	158.19 ± 0.96	-155.55 ± 0.91	158.96 ± 0.96
8	-198.24 ± 0.97	190.70 ± 1.24	-206.80 ± 0.98	199.26 ± 1.25
10	-225.42 ± 1.50	210.29 ± 0.99	-242.26 ± 1.52	227.13 ± 1.01
12	-263.71 ± 1.38	258.32 ± 0.80	-272.86 ± 1.39	267.47 ± 0.81
14	-299.51 ± 2.88	306.85 ± 0.84	-302.50 ± 2.90	309.84 ± 0.86
16	-289.99 ± 2.83	294.81 ± 3.39	-300.29 ± 2.85	305.11 ± 3.41
18	-302.27 ± 1.51	316.00 ± 3.24	-320.88 ± 1.54	334.61 ± 3.27
20	-293.03 ± 3.33	295.94 ± 3.45	-319.99 ± 3.36	322.90 ± 3.48
22	-332.72 ± 3.08	319.03 ± 4.15	-368.03 ± 3.12	354.34 ± 4.19
24	-313.13 ± 4.47	332.41 ± 2.87	-356.80 ± 4.53	376.08 ± 2.93
26	-335.75 ± 5.34	321.94 ± 4.03	-387.80 ± 5.42	373.99 ± 4.11
28	-325.59 ± 3.41	344.40 ± 6.99	-386.03 ± 3.51	404.84 ± 7.09
30	-360.00 ± 3.61	367.67 ± 3.61	-428.87 ± 3.73	436.54 ± 3.73

Spp. Table 11: *ΔG_{DLLC}, ΔG_{LPLC}, ΔG_{DLLC} - ΔG_{IC} and ΔG_{LPLC} - ΔG_{IC} for different lengths of mixed bead type polyalanine including only van der Waals (Vdw) interactions in kJ/mol, at 200k with DPPC bilayer.*

Residues	ΔG_{DL}	ΔG_{LP}	ΔG_{DL} - ΔG_{IC}	ΔG_{LP} - ΔG_{IC}
1	17.02 ± 0.48	-17.57 ± 0.37	17.02 ± 0.48	-17.57 ± 0.37
2	49.04 ± 0.76	-50.39 ± 0.82	45.80 ± 2.75	-47.15 ± 2.81
4	312.78 ±11.06	-326.62 ± 15.17	205.04 ±11.07	-218.88 ± 15.18
6	348.71 ± 7.36	-326.62 ± 15.17	231.50 ± 7.37	-209.41 ± 15.18
8	265.33 ± 7.60	-265.60 ± 15.11	230.65 ± 7.65	-230.92 ± 15.16
10	322.66 ±12.20	-324.76 ± 13.58	254.32 ±12.21	-256.42 ± 13.59
12	359.31 ±15.80	-355.80 ± 15.77	323.52 ±15.83	-320.01 ± 15.80
14	462.25 ± 4.54	-446.62 ± 10.21	418.63 ± 4.59	-403.00 ± 10.26
16	422.92 ± 3.86	-428.64 ± 5.10	371.47 ± 3.92	-377.19 ± 5.16
18	492.18 ± 8.25	-517.64 ± 7.33	432.86 ± 8.33	-458.32 ± 7.41
20	582.32 ± 5.90	-605.47 ± 4.33	515.10 ± 5.99	-538.25 ± 4.42
22	639.40 ± 8.26	-628.34 ± 1.75	564.29 ± 8.37	-553.23 ± 1.86
24	690.57 ± 5.12	-663.69 ± 4.78	607.54 ± 5.27	-580.66 ± 4.93
26	699.81 ± 6.03	-675.91 ± 7.14	608.82 ± 6.21	-584.92 ± 7.32
28	722.42 ± 4.28	-722.46 ± 9.39	622.85 ± 5.14	-622.89 ± 10.25
30	764.76 ± 5.40	-793.63 ± 6.44	650.26 ±13.92	-679.13 ± 14.96

Spp. Table 12 : *ΔG_{DL}, ΔG_{LP}, ΔG_{DL} - ΔG_{IC} and ΔG_{LP} - ΔG_{IC} for different lengths of mixed bead type polyalanine including both electrostatic (q) and van der Waals (Vdw) interactions in kJ/mol, at 300k with DOPC bilayer.*

Residues	ΔG_{DL}	ΔG_{LP}	ΔG_{DL} - ΔG_{IC}	ΔG_{LP} - ΔG_{IC}
1	15.88 ± 0.45	-17.12 ± 0.55	15.88 ± 0.45	-17.12 ± 0.55
2	50.22 ± 0.82	-49.54 ± 0.41	50.22 ± 0.82	-49.54 ± 0.41
4	136.03 ± 5.73	-136.60 ± 5.75	127.88 ± 5.74	-128.45 ± 5.76
6	116.82 ± 5.38	-119.03 ± 3.10	103.69 ± 5.39	-105.90 ± 3.11
8	138.33 ± 3.56	-138.86 ± 4.62	117.94 ± 3.58	-118.47 ± 4.64
10	183.81 ± 6.40	-175.35 ± 4.67	155.48 ± 6.42	-147.02 ± 4.69
12	214.73 ± 3.63	-202.07 ± 2.14	178.95 ± 3.67	-166.29 ± 2.18
14	240.84 ± 3.25	-226.46 ± 6.39	197.24 ± 3.29	-182.86 ± 6.43
16	260.80 ± 2.55	-278.83 ± 3.16	209.34 ± 2.61	-227.37 ± 3.22
18	281.36 ± 1.78	-299.98 ± 3.70	222.03 ± 1.86	-240.65 ± 3.78
20	333.09 ± 1.73	-332.56 ± 2.72	265.89 ± 1.83	-265.36 ± 2.82
22	350.66 ± 4.29	-363.26 ± 3.90	275.53 ± 4.41	-288.13 ± 4.02
24	402.33 ± 5.25	-408.07 ± 3.62	319.29 ± 5.40	-325.03 ± 3.77
26	434.42 ± 3.39	-425.93 ± 0.92	343.42 ± 3.56	-334.93 ± 1.09
28	468.85 ± 1.26	-467.14 ± 1.64	369.88 ± 1.45	-368.17 ± 1.83
30	497.53 ± 1.82	-501.36 ± 1.56	390.57 ± 2.06	-394.40 ± 1.80

Spp. Table 13 : *ΔG_{DL}, ΔG_{LP}, ΔG_{DL} - ΔG_{IC} and ΔG_{LP} - ΔG_{IC} for different lengths of mixed bead type polyalanine including only van der Waals (Vdw) interactions in kJ/mol, at 300k with DOPC bilayer.*

Residues	ΔG_{DLLC}	ΔG_{LPLC}	ΔG_{DLLC} - ΔG_{IC}	ΔG_{LPLC} - ΔG_{IC}
1	-71.33 ± 0.06	71.59 ± 0.14	-71.33 ± 0.06	71.59 ± 0.14
2	-106.86 ± 0.27	106.96 ± 0.17	-106.89 ± 0.17	106.96 ± 0.17
4	289.13 ± 1.85	-285.30 ± 0.69	-774.30 ± 0.20	99.32 ± 0.71
6	398.05 ± 1.64	-398.22 ± 0.74	-690.47 ± 3.40	0.83 ± 0.76
8	351.93 ± 1.64	-346.28 ± 3.12	-623.25 ± 4.41	7.75 ± 3.16
10	276.57 ± 2.84	-272.38 ± 2.90	-308.82 ± 9.06	3.13 ± 2.96
12	116.42 ± 3.30	-117.56 ± 1.78	108.29 ± 3.31	-109.43 ± 1.79
14	123.95 ± 1.46	-133.25 ± 1.86	122.19 ± 1.47	-131.49 ± 1.87
16	126.63 ± 1.22	-126.92 ± 3.13	118.08 ± 1.24	-118.37 ± 3.15
18	145.93 ± 0.78	-154.23 ± 3.14	129.58 ± 0.81	-137.88 ± 3.17
20	140.42 ± 2.86	-153.24 ± 5.31	116.24 ± 2.90	-129.06 ± 5.35
22	166.05 ± 2.09	-172.68 ± 2.03	134.02 ± 2.13	-140.65 ± 2.07
24	170.87 ± 1.78	-186.69 ± 2.43	130.98 ± 1.83	-146.80 ± 2.48
26	182.25 ± 2.59	-182.07 ± 2.05	134.50 ± 2.66	-134.32 ± 2.12
28	184.22 ± 1.72	-192.72 ± 1.12	128.39 ± 1.98	-136.89 ± 1.38
30	198.03 ± 3.68	-203.37 ± 4.80	124.83 ±3.68	-130.17 ± 3.60

Spp. Table 14 *: ΔG_{DLLC}, ΔG_{LPLC}, ΔG_{DLLC} - ΔG_{IC} and ΔG_{LPLC} - ΔG_{IC} for different lengths of mixed bead type polyalanine including both electrostatic (q) and van der Waals (Vdw) interactions in kJ/mol, at 300k with DOPC bilayer.*

Residues	ΔG_{DLLC}	ΔG_{LPLC}	ΔG_{DLLC} - ΔG_{IC}	ΔG_{LPLC} - ΔG_{IC}
1	-71.81 ± 0.12	71.59 ± 0.14	-71.81 ± 0.12	71.59 ± 0.14
2	-106.86 ± 0.27	106.96 ± 0.17	-106.86 ± 0.27	106.96 ± 0.17
4	-105.82 ± 0.38	105.90 ± 0.45	-105.82 ± 0.38	105.90 ± 0.45
6	-6.07 ± 2.34	5.06 ± 2.27	-6.43 ± 2.34	5.42 ± 2.27
8	0.67 ± 4.06	-1.40 ± 3.04	-6.97 ± 4.07	6.24 ± 3.05
10	9.57 ± 1.50	-9.93 ± 2.07	-5.83 ± 1.51	5.47 ± 2.08
12	2.81 ± 1.57	-3.20 ± 0.65	-5.32 ± 1.58	4.93 ± 0.66
14	-4.35 ± 1.05	12.84 ± 3.18	-6.12 ± 1.07	14.61 ± 3.20
16	3.31 ± 0.96	-0.19 ± 4.05	-5.24 ± 0.98	8.36 ± 4.07
18	11.32 ± 0.26	-11.35 ± 0.38	-5.03 ± 0.28	5.00 ± 0.40
20	18.98 ± 0.76	-15.10 ± 1.99	-5.21 ± 0.79	9.09 ± 2.02
22	25.89 ± 0.67	-19.63 ± 1.80	-6.14 ± 0.71	12.40 ± 1.84
24	33.29 ± 1.14	-31.09 ± 3.68	-6.62 ± 1.20	8.82 ± 3.74
26	38.34 ± 2.59	-41.50 ± 0.35	-9.44 ± 2.65	6.28 ± 0.41
28	48.83 ± 0.76	-48.31 ± 1.53	-6.81 ± 0.85	7.33 ± 1.62
30	56.67 ± 0.71	-56.40 ± 0.67	-6.88 ± 0.80	7.15 ± 0.76

Spp. Table 15 *: ΔG_{DLLC}, ΔG_{LPLC}, ΔG_{DLLC} - ΔG_{IC} and ΔG_{LPLC} - ΔG_{IC} for different lengths of mixed bead type polyalanine including only van der Waals (Vdw) interactions in kJ/mol, at 300k with DOPC bilayer.*